Bulletin of the
University of Minnesota

ENGINEERING EXPERIMENT STATION
FRANK B. ROWLEY, Director

BULLETIN NO. 14

SQUARE SECTIONS OF REINFORCED CONCRETE UNDER THRUST AND NONSYMMETRICAL BENDING

BY

PAUL ANDERSEN, Ph.D.
Assistant Professor of Structural Engineering

Vol. XLII No. 41 August 12 1939

MINNEAPOLIS

Entered at the post-office in Minneapolis as second-class matter
Minneapolis, Minnesota
Accepted for mailing at special rate of postage provided for in section 1103,
Act of October 3, 1917, authorized July 12, 1918

TABLE OF CONTENTS

ACKNOWLEDGMENTS

The research work reported in this bulletin was done in the Engineering Experiment Station of the University of Minnesota of which Professor Frank B. Rowley is the director. The plotting and drawing of all diagrams and the drawing of all illustrations were done with the assistance of personnel furnished by the Works Progress Administration, Official Project No. 665-71-3-69, Sub-project No. 303. The writer is on the staff of the Civil Engineering Department, of which Professor Frederic Bass is chairman.

SQUARE SECTIONS OF REINFORCED CONCRETE UNDER THRUST AND NONSYMMETRICAL BENDING

PURPOSE AND SCOPE

In this bulletin is presented a rational analysis of square concrete sections subjected to the action of a direct force and four bending moments as shown in Figure 1. In order to facilitate the use of the theoretical relationships between external loads and internal stresses a number of design diagrams have been worked out. These diagrams will enable the structural designer to arrive at the stresses for the most common cases without going through the solution of the equations.

In the latter part of the bulletin is presented the results of testing twenty-four square sections of reinforced concrete loaded eccentrically in two directions.

It appears from the test data that the formulas developed for nonsymmetrical bending represent the actual stress distribution with the same accuracy as the conventional analysis of reinforced concrete.

THEORETICAL INVESTIGATIONS

ASSUMPTIONS

In deriving the formulas for stresses in reinforced concrete sections under thrust and nonsymmetrical bending the following assumptions have been made:

Assumption 1. Plane sections remain plane and normal to the longitudinal fibers after bending.

Assumption 2. Both steel and concrete obey Hooke's law; that is stress intensity is proportional to strain.

Assumption 3. Tensile stresses which may exist in the concrete below the neutral axis are disregarded.

Assumption 4. The bond between the concrete and the steel is sufficient to cause the two materials to act as one.

Assumption 5. The neutral axis is perpendicular to the plane of bending.

The first four of these assumptions are those upon which conventional reinforced concrete design is based. For the purpose of simplifying the mathematical treatment and making the general case of direct stress and nonsymmetrical bending conform with the special cases, treated in the current textbooks, the fifth assumption has been made. As this assumption is not strictly correct a few remarks concerning its validity are in order.

Consider a square section of a material capable of resisting tension as well as compression. If this section is subjected to the influence of a bending moment acting in any plane through the axis of the member,

then the neutral axis, that is the line of zero stress, will be perpendicular to the plane of bending forces. In case of a composite material, such as reinforced concrete, where only the longitudinal fibers consisting of steel can be counted on for resisting tension, the neutral axis will no longer remain normal to the plane of bending. Its direction will be determined by the requirement that the sum of moments with respect to the plane of external bending must be zero. As will be shown on pages 16 and 17 of this bulletin, however, the deviation from a right angle is so small that no appreciable error is involved in assuming for a square section with symmetrical reinforcement that the neutral axis is perpendicular to the plane of bending.

In computing internal forces and moments the slight reduction in compression area of the concrete caused by the presence of the steel reinforcement has been neglected as is usually done in problems of this nature.

NOMENCLATURE

The notation, introduced in this bulletin, conforms essentially with "Symbols for Mechanics, Structural Engineering, and Testing Materials" compiled by the American Standards Association. The following symbols are used:

A_s = cross-sectional area of one reinforcing bar.
D = length of diagonal.
d = distance from corner to reinforcing bar.
e = eccentricity.
f = control cylinder strength of concrete.
f_c = maximum compressive stress in concrete.
f_s = maximum tensile stress in reinforcing bar.
k = distance from apex of compression area to neutral axis over length of diagonal.
k_1 = ratio of depth of the neutral axis in case of symmetrical bending.
M = bending moment.
n = ratio of moduli.
p = ratio of area of steel to area of concrete.
P = magnitude of load.
θ = angle of eccentricity.

DERIVATION OF FORMULAE

In Figure 1 is shown a reinforced concrete column supporting at a floor level four beams. Due to the monolithic nature of the connections each beam will transmit to the column a direct load, P_1, and a bending moment, M_1. The stresses thus produced in the column will be identical to those caused by a single concentrated load of magnitude

$$P = P_1 + P_2 + P_3 + P_4 \quad \text{.....(1)}$$

and acting at distance

$$e = \frac{\sqrt{(M_1 - M_2)^2 + (M_3 - M_4)^2}}{P_1 + P_2 + P_3 + P_4} \quad \text{.....(2)}$$

from the axis of the column. The angle of eccentricity, θ, is defined as the angle between the plane of bending and a diagonal plane of the member (Fig. 2). The angle of eccentricity can be determined from

$$\tan(45° - \theta) = \frac{M_1 - M_2}{M_3 - M_4} \quad (3)$$

Depending on the eccentricity, e, and the angle of eccentricity, θ, three distinct cases of stress distribution may occur.

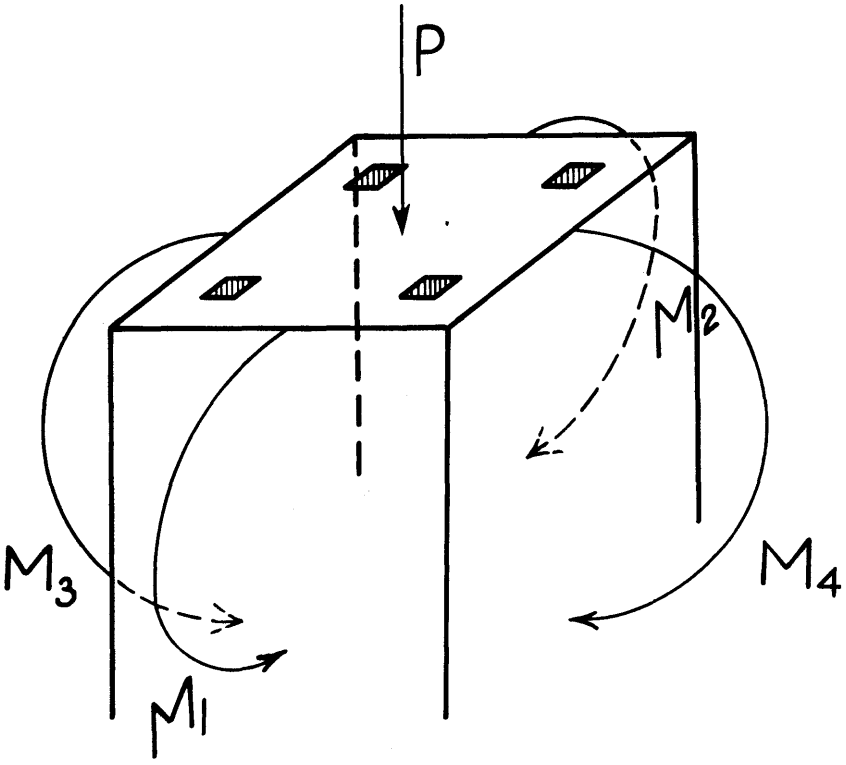

FIGURE 1. THRUST AND NONSYMMETRICAL BENDING

As shown in Figure 2, the compressive stresses may form a tetrahedral volume. This distribution is characteristic of large eccentricities and small angles of eccentricity.

As shown in Figure 3, the portion of the section which is in compression is a trapezoid. In this case the compressive stresses will form a volume which is most conveniently treated as the difference between a large tetrahedron and a small tetrahedron.

For very small eccentricities the stress distribution will be as shown in Figure 4. For the purpose of developing analytical relations, the

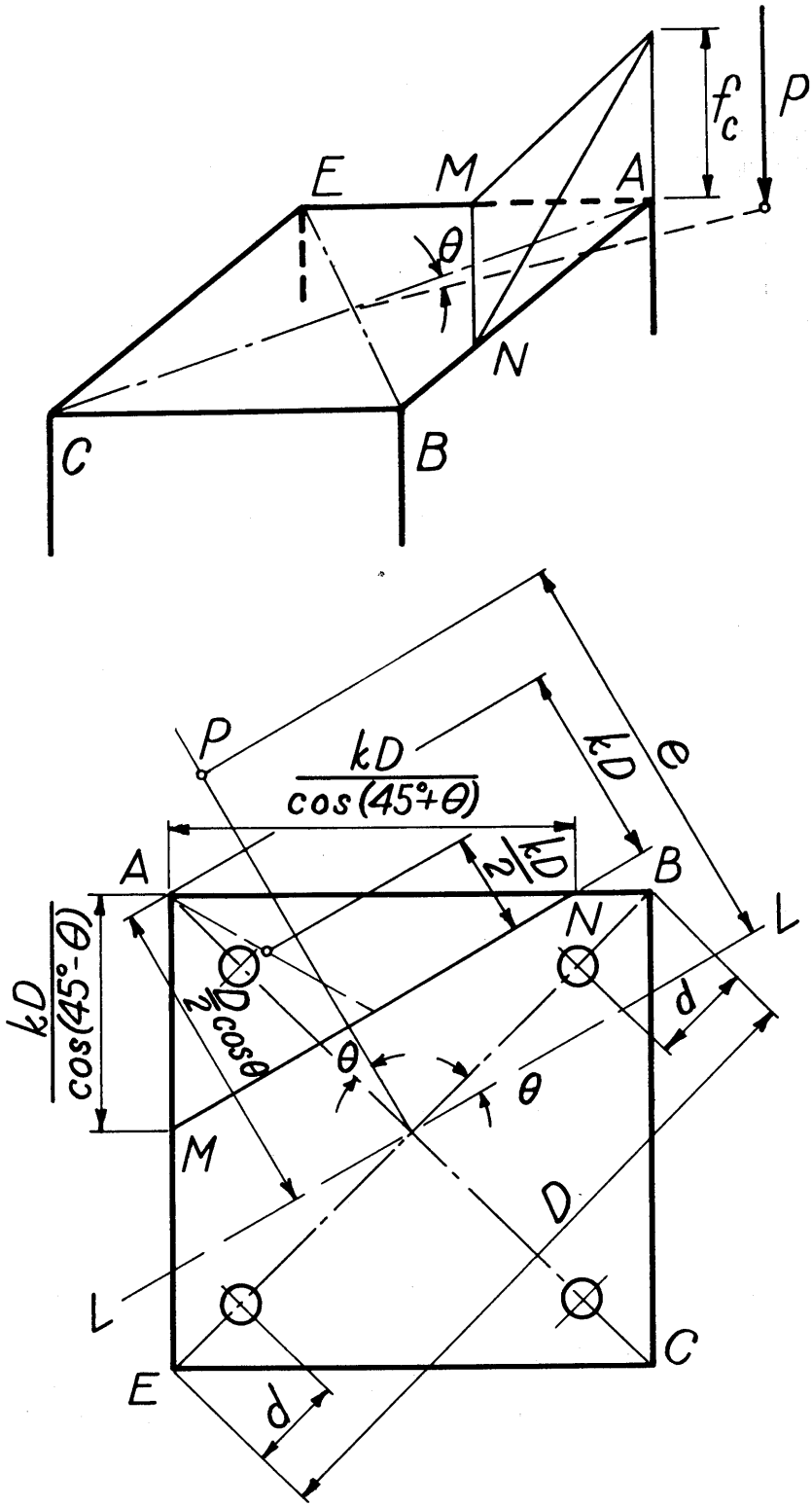

FIGURE 2. CASE A

volume of compressive stresses can be regarded as a large tetrahedron reduced by two smaller ones.

Consider a square section ABCE having compressive stresses over a triangular portion AMN and tensile stresses in three reinforcing bars (Fig. 2). The position of the neutral axis is found by eliminating P between the two equations which express respectively the equalities be-

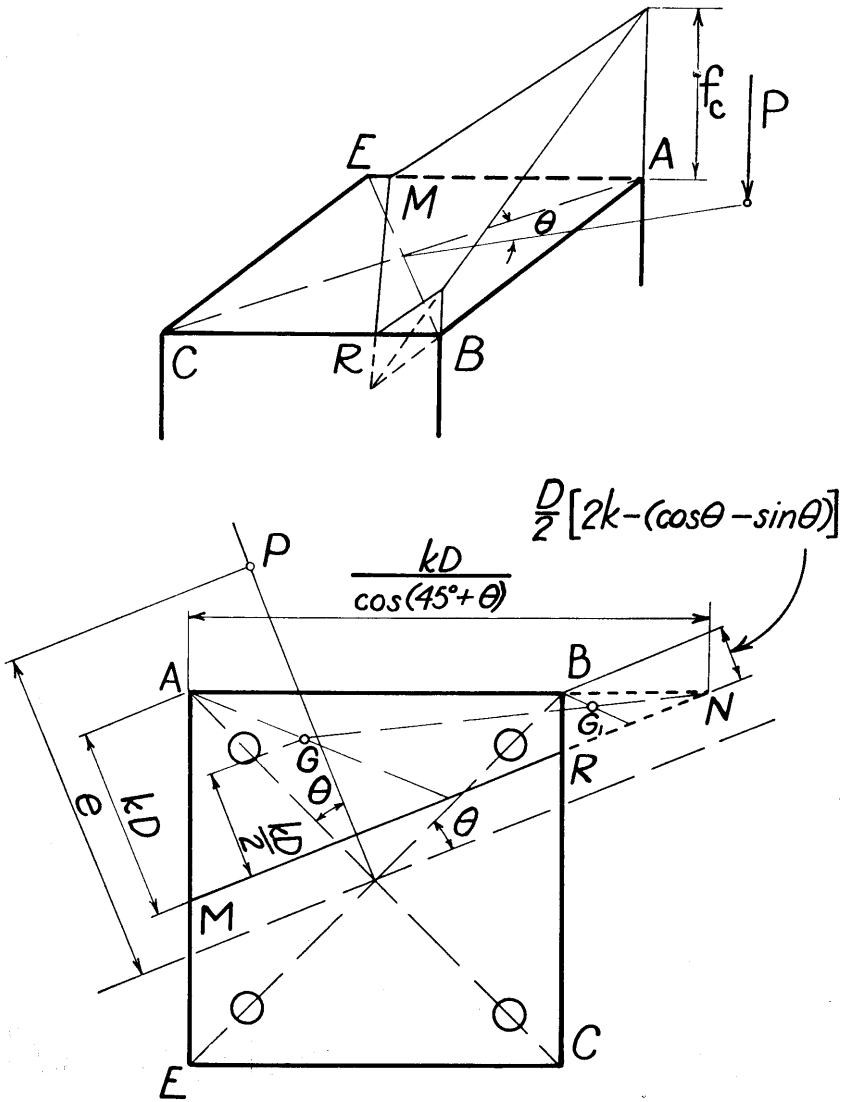

FIGURE 3. CASE B

tween the sum of internal stresses and P and the sum of internal moments and Pe, thus:

$$P = \frac{f_c}{3} \times \frac{k^2 D^2}{\cos 2\theta} + \frac{f_c\, np\, D^2}{4k} \times (2k - \cos\theta) \quad (4)$$

and

$$Pe = \frac{f_c\, k^2 D^2}{3 \cos 2\theta} \times \left(\frac{D}{2}\cos\theta - \frac{kD}{2}\right) + \frac{f_c\, np\, D^3}{4k}\left(\frac{1}{2} - \frac{d}{D}\right)^2 \quad (5)$$

Eliminating the load P between equations (4) and (5) gives for Case A

$$k^4 + k^3\left(2\frac{e}{D} - \cos\theta\right) + 3\, np \frac{e}{D}\cos 2\theta \times k - \frac{3}{2}\, np \cos 2\theta\left[\frac{e}{D}\cos\theta + \left(\frac{1}{2} - \frac{d}{D}\right)^2\right] = 0 \quad (6)$$

Solving equation (4) with respect to the maximum compressive stress, f_c, gives for Case A:

$$f_c = \frac{P}{D^2} \times \frac{12k \cos 2\theta}{4k^3 + 3\, np\, (2k - \cos\theta) \cos 2\theta} \quad (7)$$

It appears from an examination of Figure 2 and Figure 3 that if

$$\frac{\cos\theta - \sin\theta}{2} < k < \frac{\cos\theta + \sin\theta}{2} \quad (8)$$

then the compressive stresses will be distributed over a trapezoid ABRM as shown in Figure 3, where G indicates the projection of the centroid of the tetrahedron having AMN for a base and G_1 is the projection of the centroid of the smaller tetrahedron having BRN for a base. For Case B the two equations expressing equilibrium of forces and moments, are

$$P = \frac{f_c}{3} \times \frac{k^2 D^2}{\cos 2\theta}\left[1 - \left(1 - \frac{\cos\theta - \sin\theta}{2k}\right)^3\right] + \frac{f_c\, np\, D^2}{4k}\left(2k - \cos\theta\right) \quad (9)$$

and

$$Pe = \frac{f_c\, np\, D^3}{4k}\left(\frac{1}{2} - \frac{d}{D}\right)^2 + \frac{f_c\, k^2 D^2}{3 \cos 2\theta}\left(\frac{D}{2}\cos\theta - \frac{kD}{2}\right) + \frac{f_c\, k^2 D^2}{3 \cos 2\theta}\left(1 - \frac{\cos\theta - \sin\theta}{2k}\right)^3 \times \frac{D}{2}\left(k - \frac{\cos\theta + \sin\theta}{2}\right) \quad (10)$$

Eliminating P between (9) and (10) gives an equation from which the position of the neutral axis can be determined for Case B, namely:

$$k^3 + \left(3\frac{e}{D} - \frac{3}{2}\cos\theta\right)k^2 - \frac{\cos\theta - \sin\theta}{4}\left[6\frac{e}{D} - 2\cos\theta - \sin\theta\right]k + 3\, np \frac{e}{D}(\cos\theta + \sin\theta)\, k - \frac{3}{2}(\cos\theta + \sin\theta)\, np\left[\frac{e}{D}\cos\theta + \left(\frac{1}{2} - \frac{d}{D}\right)^2\right] + \frac{(\cos\theta - \sin\theta)^3}{16}\left[4\frac{e}{D} - \cos\theta - \sin\theta\right] = 0 \quad (11)$$

Solving equation (9) for f_c gives the maximum compressive stress for Case B.

$$f_c = \frac{P}{D^2} \times \frac{24k\,(\cos\theta + \sin\theta)}{12k^2 - 6\,(\cos\theta - \sin\theta)\,k + (\cos\theta - \sin\theta)^2 + 6\,np\,(2k - \cos\theta)\,(\cos\theta + \sin\theta)} \quad \text{.....(12)}$$

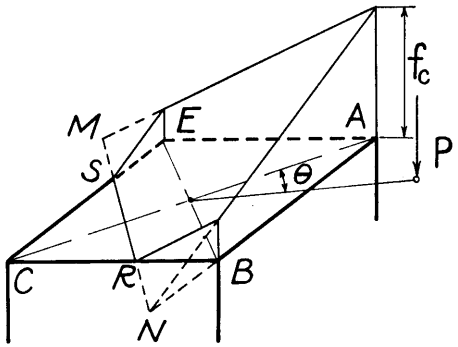

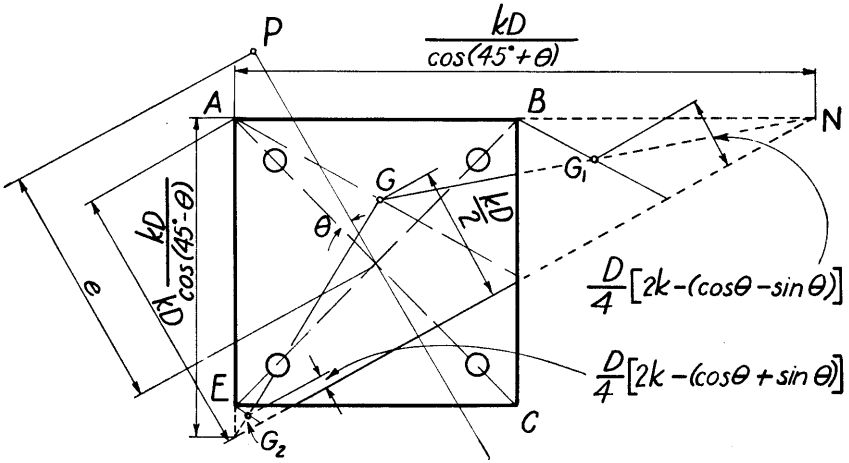

FIGURE 4. CASE C

For Case C, shown in Figure 4, the two equations expressing zero sum of forces and moments, are

$$P = \frac{f_c k^2 D^2}{3\cos 2\theta}\left[1 - \left(1 - \frac{\cos\theta - \sin\theta}{2k}\right)^3 - \left(1 - \frac{\cos\theta + \sin\theta}{2k}\right)^3\right] + \frac{f_c\,np\,D^2}{4k}\left(2k - \cos\theta\right) \quad \text{.....(13)}$$

and

$$Pe = \frac{f_c\, np\, D^3}{4k}\left(\frac{1}{2} - \frac{d}{D}\right)^2 + \frac{f_c\, k^2 D^2}{3\cos 2\theta}\left(\frac{D}{2}\cos\theta - \frac{kD}{2}\right)$$
$$+ \frac{f_c\, k^2 D^2}{3\cos 2\theta}\left(1 - \frac{\cos\theta - \sin\theta}{2k}\right)^3 \times \frac{D}{2}\left(k - \frac{\cos\theta + \sin\theta}{2}\right)$$
$$+ \frac{f_c k^2 D^2}{3\cos 2\theta}\left(1 - \frac{\cos\theta + \sin\theta}{2k}\right)^3 \times \frac{D}{2}\left(k - \frac{\cos\theta - \sin\theta}{2}\right) \quad (14)$$

For Case C the position of the neutral axis is found from

$$k^4 + \left(2\frac{e}{D} - 3\cos\theta\right)k^3 + 3\cos\theta\left(\cos\theta - 2\frac{e}{D}\right)k^2$$
$$-\left[\cos^3\theta + 3\frac{e}{D}(np\cos 2\theta - 1)\right]k - \frac{e}{2D}\cos\theta\,(1 + 2\sin^2\theta) + \frac{\cos 2\theta}{8}$$
$$+\frac{3}{2}np\cos 2\theta\left[\frac{e}{D}\cos\theta + \left(\frac{1}{2} - \frac{d}{D}\right)^2\right] = 0 \quad (15)$$

and the greatest unit compressive fiber stress is

$$f_c = \frac{P}{D^2} \times \frac{12k\cos 2\theta}{-4k^3 + 12k^2\cos\theta - 6k + \cos\theta\,(1 + 2\sin^2\theta) + 3np\,(2k - \cos\theta)\cos 2\theta} \quad (16)$$

Maximum tension will occur in the reinforcing bar most distant from the neutral axis and will equal

$$f_s = nf_c\left[\left(1 - \frac{d}{D}\right)\frac{\cos\theta}{k} - 1\right] \quad (17)$$

SPECIAL CASES

It is of interest to examine the formulas for several special cases. If the section is subjected to the action of two unequal bending moments unaccompanied by thrust the position of the neutral axis can be determined directly from the equation expressing zero sum of all internal stresses, or by making $\frac{e}{D}$ approach infinity in the general equations. In case of nonsymmetrical bending alone it is readily shown that only Case A and Case B are possible, the transition between the two cases taking place when

$$k = \frac{1}{2}(\cos\theta - \sin\theta) \quad (18)$$

The equations from which k may be determined are for Case A,

$$k^3 + \frac{3}{2}np\cos 2\theta \times k - \frac{3}{4}np\cos\theta\cos 2\theta = 0 \quad (19)$$

and for Case B,

$$k^2 - \left[\frac{\cos\theta - \sin\theta}{2} - np\,(\cos\theta + \sin\theta)\right]k + \frac{(\cos\theta - \sin\theta)^2}{12}$$
$$-\frac{np}{2}\cos\theta\,(\cos\theta + \sin\theta) = 0 \quad (20)$$

The maximum compressive stress is found for Case A from the relation

$$f_c = \frac{M}{D^3} \times \frac{12k \cos 2\theta}{2k^3 (\cos\theta - k) + 3np\left(\frac{1}{2} - \frac{d}{D}\right)^2 \cos 2\theta} \quad (21)$$

and for Case B from

$$f_c = \frac{M}{D^3} \times \frac{12k \cos 2\theta}{k^3\left[2\cos\theta - 2k - \left(1 - \frac{\cos\theta - \sin\theta}{2k}\right)^3 (\cos\theta + \sin\theta - k)\right] + 3pn\left(\frac{1}{2} - \frac{d}{D}\right)^2 \cos 2\theta} \quad (22)$$

where

$$M = \sqrt{M_1^2 + M_2^2} \quad (23)$$

If $M_1 = M_2$ then the total bending moment will act in a plane through one of the diagonals. For this case of diagonal bending the neutral axis may be determined from

$$k^3 + \frac{3}{2} pnk - \frac{3}{4} pn = 0 \quad (24)$$

and the maximum compressive stress

$$f_c = \frac{M}{D^3} \frac{6k}{k^3 (1-k) + \frac{3}{2} pn\left(\frac{1}{2} - \frac{d}{D}\right)^2} \quad (25)$$

Maximum tension which will occur in the bar most distant from the neutral axis equals

$$f_s = nf_c\left(\frac{1-k}{k} - \frac{d}{kD}\right) \quad (26)$$

An important application of this case of diagonal bending is the determination of handling stresses in precast concrete piles which are generally lifted in such a way that one diagonal of the square cross section becomes horizontal. In this position the bending moment to be resisted by the section will act in a plane through the vertical diagonal. Compressive stresses thus set up can be computed as explained above.

If the section is subjected to the action of a direct concentric load and two equal bending moments, the stresses in the member will be identical with those caused by a single concentrated load acting at a point on the diagonal. In this case the neutral axis will be parallel to the other diagonal. Depending on the eccentricity of the equivalent single force, the neutral axis may be above this diagonal corresponding to Case A; or it may lie below corresponding to Case C. For this condition of thrust combined with diagonal bending Case B disappears and the position of the neutral axis can be determined from Case A, ($k < \frac{1}{2}$),

$$k^4 + k^3\left(2\frac{e}{D} - 1\right) + 3pn\frac{e}{D}k - \frac{3}{2}pn\left[\frac{e}{D} + \left(\frac{1}{2} - \frac{d}{D}\right)^2\right] = 0 \quad (27)$$

and for Case C, ($k > \frac{1}{2}$),

$$k^4 + k^3\left(2\frac{e}{D} - 3\right) - k^2\left(6\frac{e}{D} - 3\right) - k\left[1 - 3\frac{e}{D}\left(1 - pn\right)\right] + \frac{1}{8} - \frac{e}{2D} + \frac{3}{2}pn\left[\frac{e}{D} + \left(\frac{1}{2} - \frac{d}{D}\right)^2\right] = 0 \quad (28)$$

The maximum compressive stress is determined from for Case A

$$f_c = C_A \frac{P}{D^2} \quad (29)$$

in which

$$C_A = \frac{12k}{4k^3 + 6\,pnk - 3\,pn} \quad (30)$$

and for Case C

$$f_c = C_C \frac{P}{D^2} \quad (31)$$

in which

$$C_C = \frac{12k}{-4k^3 + 12k^2 + 6k\,(pn - 1) + 1 - 3\,pn} \quad (32)$$

DESIGN DIAGRAMS

The variation of k as a function of $\frac{e}{D}$ is shown in Figure 5, the angle of eccentricity is $\theta = 22\frac{1}{2}°$ and the ratio of embedment $\frac{d}{D} = .2$. It should be noted that the rate of change of k is very great when $\frac{e}{D}$ becomes small; for design purposes it is therefore advisable to express graphically k as a function of the reciprocal $\frac{D}{e}$. This has been done in Diagrams 1, 2, 3, 4, and 5 where for a ratio of embedment, $\frac{d}{D} = .2$, k has been plotted for angles of eccentricity of 0°, 10°, 20°, 30°, and 40°. To provide for the various values of n, the quantity pn has been used as an argument instead of n.

The purpose of Diagram 6 is to enable the designer to determine for any given data which of the three cases A, B, or C will represent the stress distribution on the section and which of the three Equations (6), (11), or (15) should be used for determining the position of the neutral axis. Two ratios of embedment have been assumed, namely, $\frac{d}{D} = .1$ and $\frac{d}{D} = .2$. The two dotted lines at the upper corners of the two diagrams represent values for which no tension will exist in the reinforcing bars.

The purpose of Diagrams 7, 8, 9, 10, and 11 is to assist in computing maximum compressive stresses in the concrete. It will be recalled that this stress can be expressed thus:

$$f_c = C\frac{P}{D^2} \quad (33)$$

where the expression for C is dependent on the case of stress distribution as indicated by Equations (7), (12), and (16). The reciprocal of C as a function of $\frac{D}{e}$ is shown on Diagrams 7, 8, 9, 10, and 11 for angles of eccentricity of 0°, 10°, 20°, 30°, and 40°, respectively.

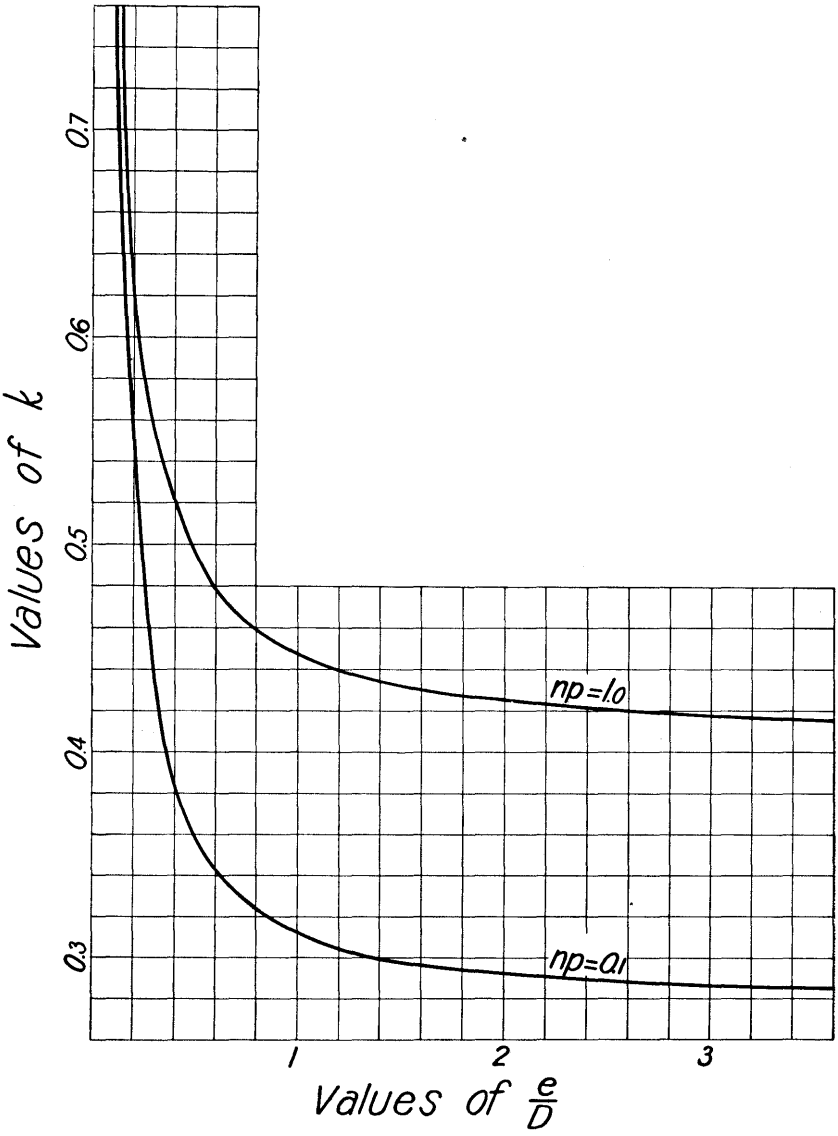

FIGURE 5. VARIATION OF k FOR $\theta = 22\frac{1}{2}°$, $\frac{d}{D} = 0.2$

NUMERICAL EXAMPLE

As an illustration of the practical application of the foregoing analysis consider the column section shown in Figure 6, the longitudinal reinforcement of which consists of four one-inch square steel bars. The modular ratio, n, is assumed to be equal to ten. The section is subjected to the influence of a direct load $P = 11{,}900$ pounds and two bending moments $M_1 = 152{,}000$ inch-pounds and $M_2 = 197{,}200$ inch-pounds acting in the two principal planes.

The stresses produced in the column will be identical to those produced by a single load $P = 11{,}900$ pounds acting at a distance

$$e = \frac{\sqrt{152{,}000^2 + 197{,}200^2}}{11{,}900} = 20.92'' \qquad (34)$$

from the center line of the column and lying in a plane making an angle, θ, with one of the diagonals which can be determined from the relation

$$\tan (45^\circ + \theta) = \frac{1972}{1520} = 1.2974$$

$$\theta = 7^\circ\ 24\tfrac{1}{2}' \qquad (35)$$

Other quantities to be computed are

$$\frac{d}{D} = 0.2 \qquad \frac{e}{D} = \frac{20.92}{21.21} = 0.9862 \qquad \frac{D}{e} = 1.014$$

$$p = 0.0178 \qquad pn = 0.178 \qquad (36)$$

An examination of Diagram 6 will reveal that for the above values of θ, $\frac{D}{e}$ and pn the stress distribution will be according to Case A. Substituting in Equation (6) gives

$$k^4 + 0.98075\,k^3 + 0.50912\,k - 0.27566 = 0 \qquad (37)$$

solving by trial gives $k = .386$. The maximum compressive stress is, according to (7)

$$f_c = \frac{11{,}900}{450} \times \frac{12 \times .386 \times .96675}{4 \times .386^3 + .534 \times (2 \times .386 - .99165) \times .96675}$$

$$f_c = 1{,}015 \text{ lb. per sq. in.} \qquad (38)$$

The maximum tensile stress in the steel reinforcement is according to (17)

$$f_s = 10{,}150 \times \left(0.8\,\frac{.99165}{.386} - 1\right)$$

$$f_s = 10{,}710 \text{ lb. per sq. in.} \qquad (39)$$

These can be approximated by making use of the design diagrams. Thus from Diagram 1 ($\theta = 0^\circ$) it is found that, for $\frac{D}{e} = 1.014$ and pn $= .178$, $k = .39$. And from Diagram 2 ($\theta = 10^\circ$) that for the same values $k = .38$. Interpolating gives for $\theta = 7^\circ\ 24'$, $k = .383$.

Similarly from Diagram 8 ($\theta = 0°$) and Diagram 9 ($\theta = 10°$) for the maximum compressive stress.

$$f_c = \frac{11{,}900}{450} \div 0.026 = 1{,}120 \text{ lb. per sq. in.} \quad (40)$$

It has been stated previously in this bulletin that the assumption of perpendicularity between the plane of bending and the neutral axis is not strictly correct. A discussion of the error involved in this assumption is given in the following.

The conditions of equilibrium of parallel forces in space are that the summation of the magnitudes must equal zero, and also that the summation of the moments of the forces about each of two lines lying in a perpendicular plane must equal zero. Only two of these requirements were used in deriving the formulas in this bulletin.

The eccentric load in this example was determined by assuming a neutral axis (called "actual neutral axis" in Fig. 6) and a maximum

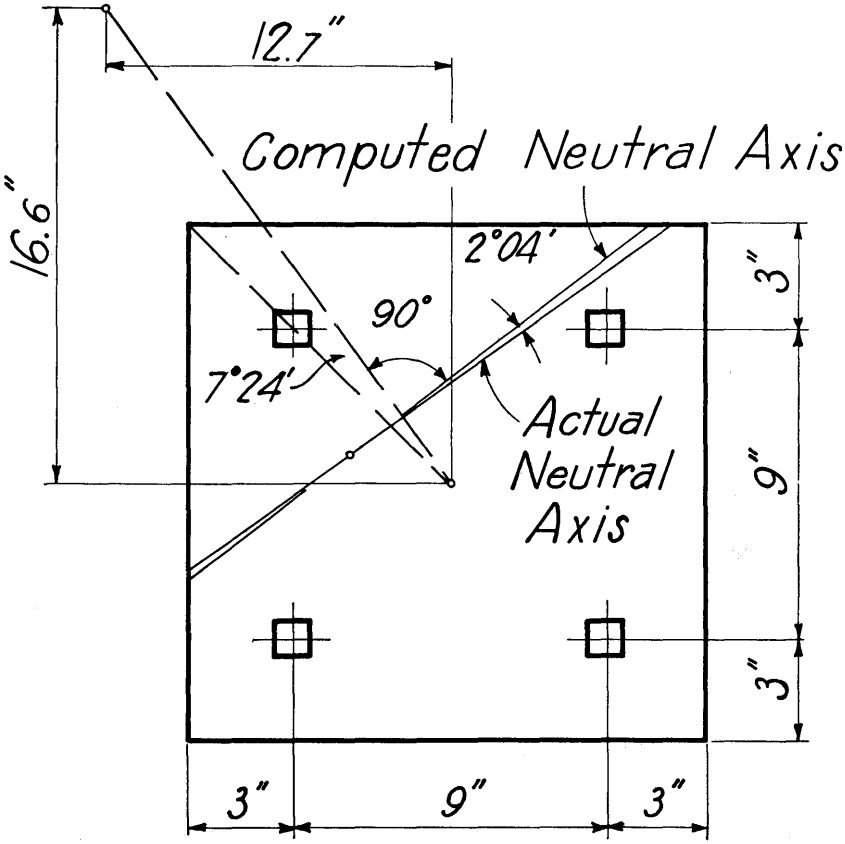

FIGURE 6. NUMERICAL EXAMPLE

compressive stress in the concrete of 1,000 pounds per square inch. Stresses in the reinforcing bars, which are proportional to the distances to the actual neutral axis, were then computed, and the corresponding eccentric load determined by the three requirements of statics. The first of these equations, expressing zero sum of all vertical forces, contains only one unknown, namely, the magnitude of the eccentric load. Co-ordinates to the point of eccentricity were then determined by the two moment equations.

Figure 6 shows the close agreement between the actual neutral axis and the neutral axis computed by the analysis presented in this bulletin. The stresses in the concrete and the steel compare as follows:

Actual:	$f_c = 1{,}000$	$f_s = 10{,}570$
Computed:	$f_c = 1{,}015$	$f_s = 10{,}710$

It is of interest to note that the computed stresses are slightly on the safe side.

EXPERIMENTAL INVESTIGATIONS

APPARATUS AND TEST SPECIMENS

The testing of twenty-four specimens loaded eccentrically in two directions will be reported in this bulletin.

Figure 7 shows the make-up of the specimens which were all of the same cross section but reinforced with varying amounts of longitudinal steel. The first group (Specimens 1 to 6, inclusive) had four ⅜-inch round bars, the second group (7 to 12) had four ½-inch round bars, the third group (13 to 18) had four ⅝-inch rounds and the fourth group (19 to 24) had four ¾-inch rounds. All longitudinal reinforcing bars were milled to exact lengths and perfect end bearing was insured by using steel end plates in the forms. Local failures at the ends, due to bending and shear, and at the fillet, due to high stress concentration, were prevented by additional reinforcement as shown in Figure 7.

The Portland cement used in manufacturing the concrete passed the standard specifications of the American Society for Testing Materials. Owing to the small clearances between reinforcement and forms, coarse aggregate was omitted and the concrete, machine-mixed for two minutes, was made with sand having a fineness modulus of 3.2.

A control cylinder six inches in diameter and twelve inches high was made from each batch and tested for modulus of elasticity and ultimate strength. The modulus of elasticity was determined from stress-strain diagrams plotted from strain gage readings. On the vertical side of the cylinder, steel plugs were grouted in the concrete for three sets of gage readings 120° apart on the circumference. The modulus of elasticity as determined in this manner showed little variation from the average value of 3,100,000 pounds per square inch. The control cylinder strengths are listed in Table I.

The reinforcement consisted of intermediate grade steed. It was subjected to the usual standard tensile tests, the results of which were 43,000 pounds per square inch for the yield point and 62,500 pounds per square inch for the ultimate strength.

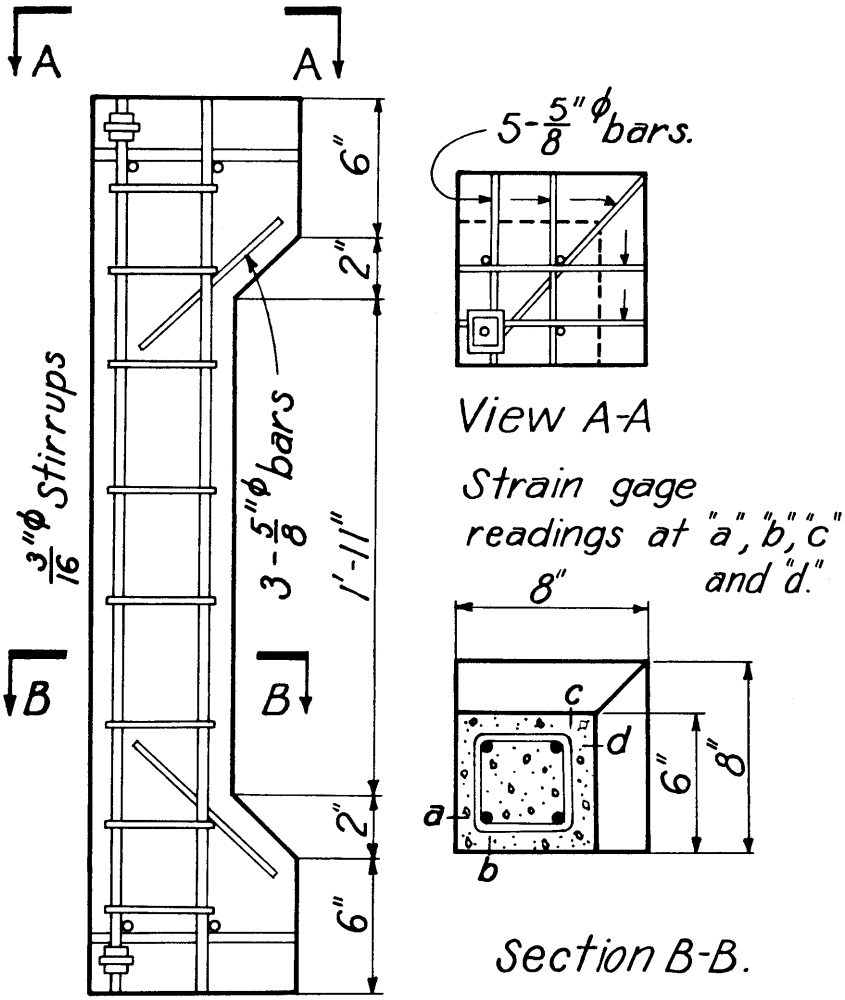

FIGURE 7. TEST SPECIMEN

The specimens as well as the control cylinders were dry cured and tested at the age of seven days. A standard testing machine with a capacity of 200,000 pounds was used. The load was applied through a spherical head consisting of a steel ball with a diameter of one inch, placed on top of the specimen while the bottom of the specimen rested directly

on the lower head of the testing machine. Desired eccentricities in two directions were obtained by placing the spherical head correspondingly.

Four strain-gage readings were taken for each load increment. As indicated in Figure 7, two of these readings were near the edge having maximum compressive stress and two at the longitudinal reinforcing bar most highly stressed in tension. Steel plugs for the drilled strain-gage holes were set and grouted in the concrete three days before the day of testing. Thus, both compressive and tensile stresses were computed from measured concrete strains.

TEST DATA

As indicated in Table I three different angles of eccentricity were investigated, namely $\theta = 0°$; $\theta = 22\frac{1}{2}°$, and $\theta = 45°$ corresponding to direct stress combined with diagonal bending (due to a couple acting in diagonal plane), unsymmetrical bending and symmetrical bending, respectively. Two different eccentricities were used with each angle.

Maximum tensile stresses in the reinforcement and maximum compressive stresses in the concrete were estimated by multiplying the strains measured by strain gage by 29,000,000 and 3,100,000, respectively (the elastic moduli for steel and concrete). These observed stresses were compared to the stresses computed by the theoretical formulas developed in this bulletin. The comparison is shown on Diagrams 12 to 23, inclusive, for the twenty-four specimens. On these diagrams C denotes the ratio between the computed and observed compressive stresses, f_c, and S denotes the ratio between the computed and observed tensile stresses, f_s. The computed stresses will, of course, vary with the load according to a straight line. The observed stresses appear to vary according to some curved line lying below the straight line. It should be noted, however, that the measured stresses in the diagrams are based on the secant modulus of elasticity at one-half the ultimate strength of the control cylinders. Also at the age of seven days, concrete possesses considerable plastic flow. Actual compressive stresses are, therefore, probably somewhat lower than indicated for the higher loads. This higher value of the modular ratio, n, at stresses near the ultimate load would also lower the value of the stresses computed from the theoretical relations.

It is important that the gap between calculated stresses and measured stresses is about the same for the cases of symmetrical bending and unsymmetrical bending. The computations of stresses for the former are based on formulas generally accepted in the analysis of reinforced concrete, for the latter on the extension of these formulas to the general case of thrust accompanied by two unequal bending moments as presented in this paper.

ULTIMATE STRENGTH

As shown in Figure 7 the test pieces were built so short that failure was not influenced by column action. After each load increment was applied and before strain-gage readings were taken the specimen was

examined closely in order to detect tension cracks. Generally these cracks became visible shortly before the ultimate load was reached. All failures, however, appeared to be compression failures. In case of diagonal bending (two equal bending moments) crushing took place at the corner as shown on specimens 1 and 2 in Figure 8. Specimen 4 was subjected to two unequal bending moments and crushing occurred at the corner and extending toward the plane of the larger bending moment as shown in Figure 8. Specimens 6 and 17 were subjected to symmetrical bending

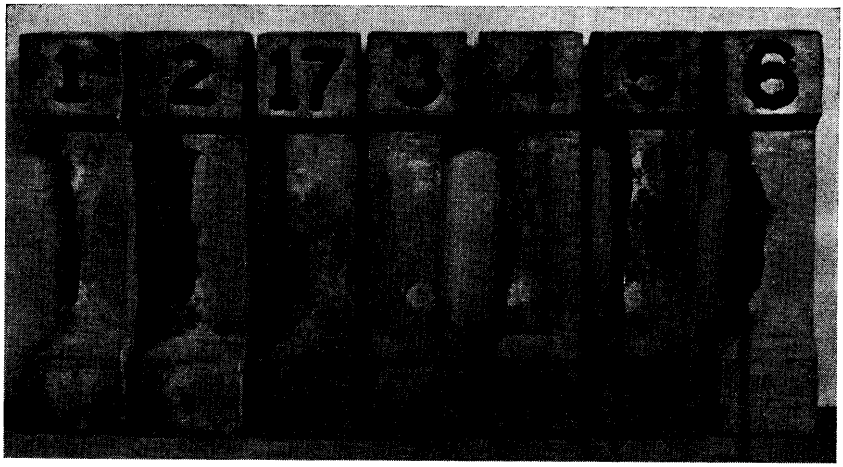

FIGURE 8. TYPES OF FAILURES

and the crushed area appears to coincide with the most highly stressed portion of the section.

The failures shown in Figure 8 were typical of the entire investigation; they indicate that the stress distribution is essentially as given by the theoretical formulas developed in this paper.

In Table II are listed maximum compressive and tensile stresses computed from the ultimate loads by the theoretical formulas. The compressive stresses appear to be considerably higher than those developed by the corresponding control cylinders, but this margin becomes smaller for increasing percentages of reinforcing.

The maximum tensile stress in the most highly stressed reinforcing bar is listed for each specimen in the last column of Table II. Except in four cases these stresses are below the yield point of the steel.

SUMMARY AND CONCLUSIONS

Design formulas for the square concrete section with symmetrical reinforcement subjected to a direct load and two unequal bending moments can be developed if, in addition to the usual assumptions of reinforced concrete design, it is assumed that the neutral axis is per-

pendicular to the plane of combined bending. These formulas include as a special case the square concrete section under direct load and one bending moment.

The general formulas give results which are consistent with those obtained for the special case of a direct load and symmetrical bending.

Applied to short members reinforced with various percentages of steel, the theoretical stresses are somewhat higher than the measured stresses.

The theoretical stresses, f_c, computed from the ultimate loads are considerably greater than the stresses, f, developed by the corresponding control cylinders. This phenomenon of a higher theoretical ultimate stress has been observed frequently in flexure tests on reinforced concrete.†

The ratio $f_c \div f$ appears to decrease with increasing percentages of reinforcing steel.

† See for instance Turneaure and Maurer: Principles of Reinforced Concrete Construction, 1932; p. 89.

TABLE I

TEST SPECIMENS

Specimen	p Per Cent	pn	θ Degrees	e Inches	Observed Control Cyl. Strength—f Lb. per Sq. In.	Ultimate Load on Specimen—P. Lb.
1	1.22	0.114	0	3.50	3,980	36,250
2	"	"	0	2.25	3,980	66,520
3	"	"	22½	2.75	3,750	50,940
4	"	"	22½	1.75	3,750	81,250
5	"	"	45	2.50	4,020	73,890
6	"	"	45	1.63	4,020	100,490
7	2.18	0.204	0	3.50	3,950	33,680
8	"	"	0	2.25	3,950	61,380
9	"	"	22½	2.75	4,170	60,010
10	"	"	22½	1.75	4,170	90,930
11	"	"	45	2.50	3,840	75,290
12	"	"	45	1.63	3,840	101,230
13	3.41	0,319	0	3.50	4,010	38,700
14	"	"	0	2.25	4,010	58,770
15	"	"	22½	2.75	3,920	52,910
16	"	"	22½	1.75	3,920	69,810
17	"	"	45	2.50	3,790	77,690
18	"	"	45	1.63	3,790	103,930
19	4.91	0,459	0	3.50	4,080	40.600
20	"	"	0	2.25	4,080	70,290
21	"	"	22½	2.75	3,970	68,350
22	"	"	22½	1.75	3,970	100,290
23	"	"	45	2.50	3,840	81,080
24	"	"	45	1.63	3,840	113,940

TABLE II

COMPARISON OF TEST DATA

Specimen	θ Degrees	Location of Neutral Axis	F_s Computed from P Lb. per Sq. In.	$\frac{F_c}{F}$	F_s Computed from P Lb. per Sq. In.
1	0	k=.443	8,668	2.18	65,310
2	0	.542	8,596	2.16	38,260
3	22½	.443	8,363	2.23	52,260
4	22½	.588	7,829	2.09	18,810
5	45	k_1=.499	8,238	2.05	46,460
6	45	.725	7,013	1.74	6,780
7	0	k=.478	6,544	1.66	41,220
8	0	.564	7,268	1.84	28,430
9	22½	.476	8,232	1.97	42,540
10	22½	.603	8,137	1.95	17,170
11	45	k_1=.545	7,235	1.88	31,650
12	45	.742	6,428	1.67	4,700
13	0	k=.503	6,301	1.57	34,820
14	0	.582	6,019	1.50	21,820
15	22½	.501	6,196	1.58	27,530
16	22½	.616	5,831	1.49	10,900
17	45	k_1=.578	6,492	1.71	23,310
18	45	.756	5,956	1.57	3,240
19	0	k=.522	5,612	1.38	27,950
20	0	.595	6,354	1.56	20,470
21	22½	.519	6,902	1.74	27,370
22	22½	.626	7,614	1.92	12,850
23	45	k_1=.604	5,917	1.54	17,950
24	45	.768	5,810	1.51	2,260

TABLE III

STRESS RATIOS

Specimen	Per Cent of Ultimate Load	C*	S*	Specimen	Per Cent of Ultimate Load	C*	S*
1	82	1.32	1.25	13	93	1.51	1.27
2	79	1.34	1.45	14	66	1.31	1.52
3	78	1.41	1.27	15	94	1.39	1.30
4	85	1.37	1.38	16	79	1.50	1.22
5	82	1.45	1.31	17	81	1.43	1.29
6	89	1.48	1.29	18	83	1.37	1.24
7	95	1.51	1.22	19	85	1.45	1.21
8	81	1.36	1.29	20	86	1.62	1.19
9	81	1.42	1.35	21	88	1.39	1.17
10	84	1.45	1.31	22	80	1.42	1.31
11	92	1.37	1.27	23	87	1.40	1.25
12	87	1.60	1.35	24	79	1.47	1.22

* C and S denote ratios between computed stresses (using load at which the last strain-gage measurements were taken) and stresses figured for these readings.

DIAGRAM 1

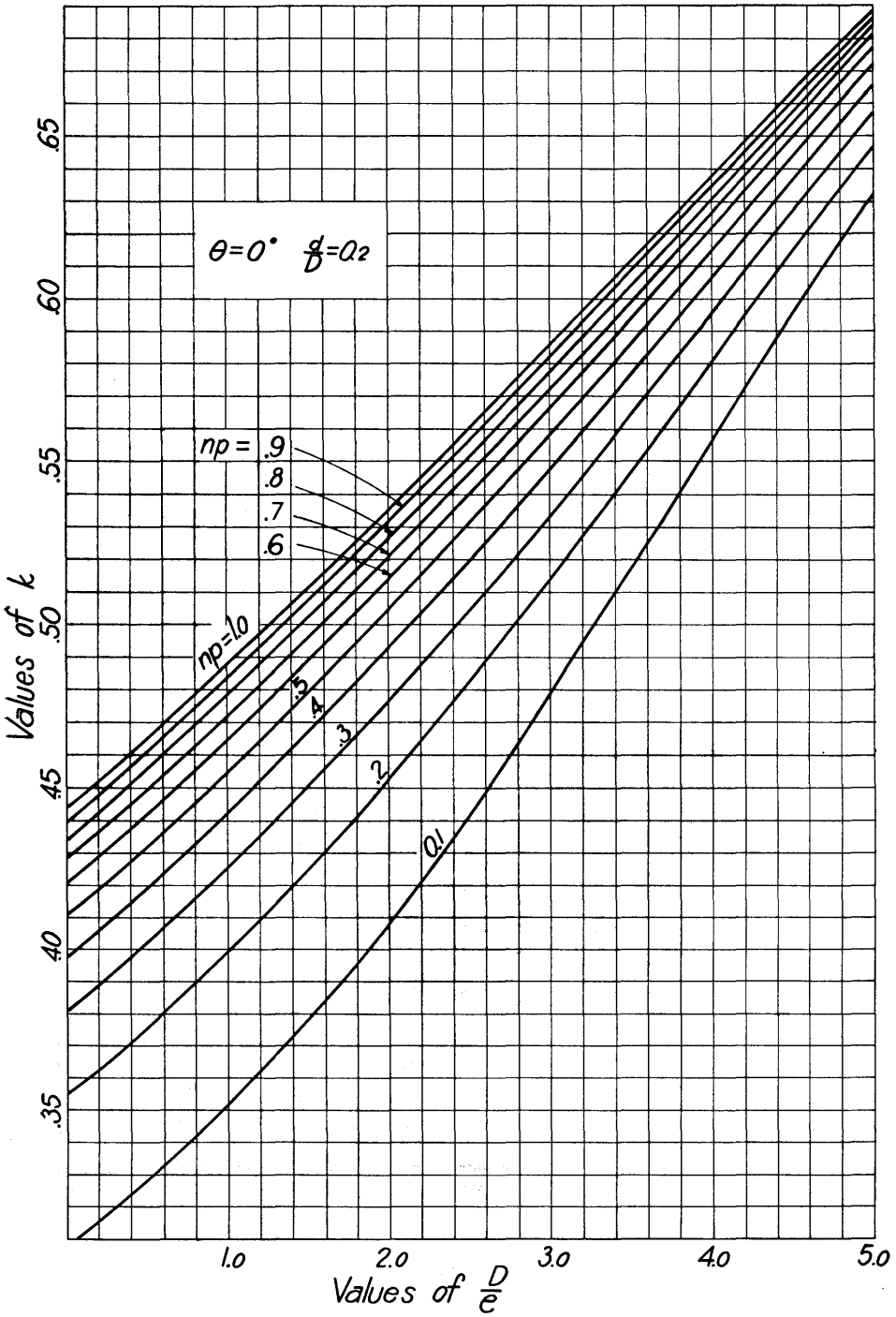
θ=0° d/D=0.2
np = .9
.8
.7
.6
np=1.0
.5
.4
.3
.2
0.1
Values of k
.35
.40
.45
.50
.55
.60
.65
1.0
2.0
3.0
4.0
5.0
Values of D/e

DIAGRAM 2

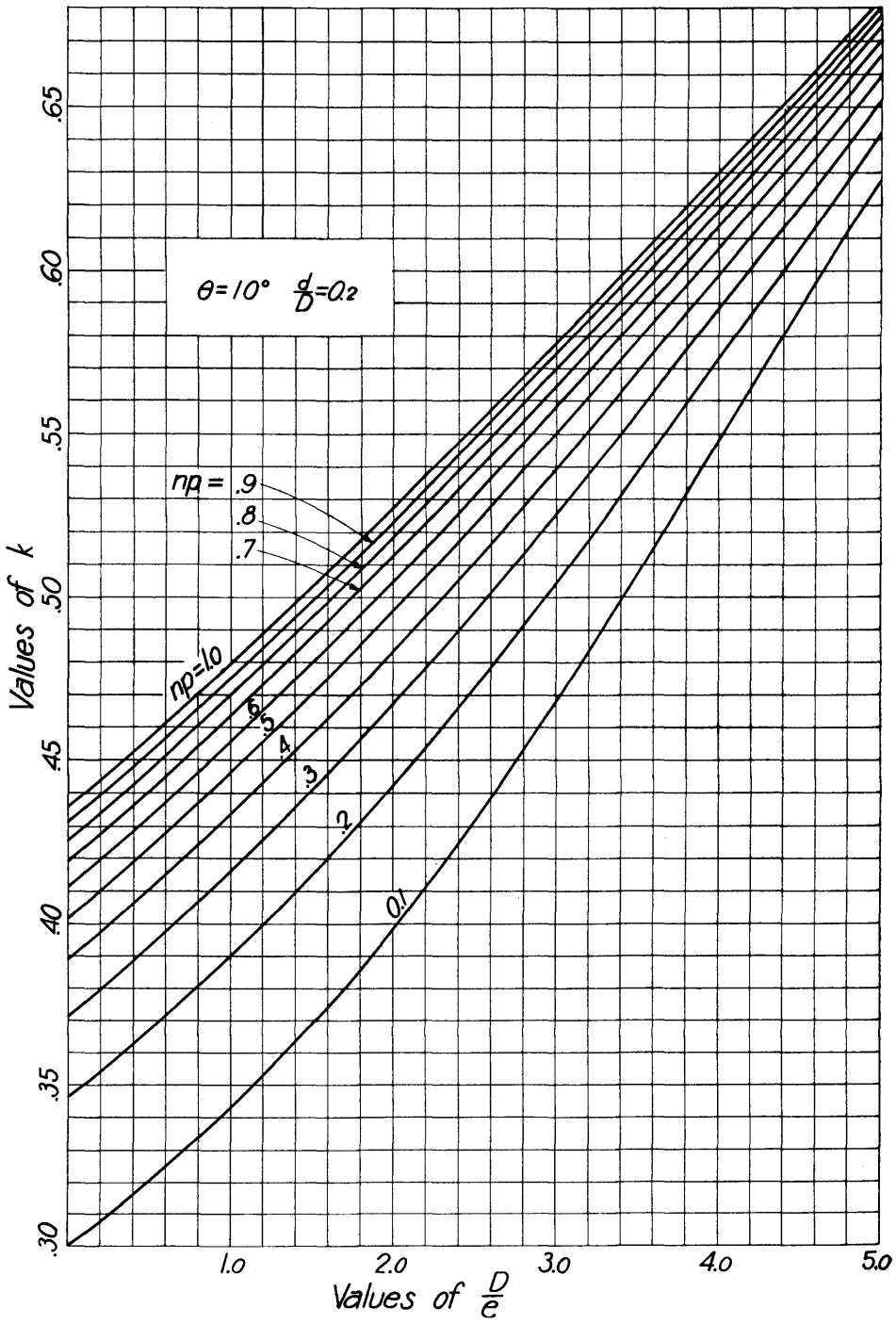
θ=10° d/D=0.2
np = .9
.8
.7
np=1.0
.6
.5
.4
.3
.2
0.1
Values of k
.30
.35
.40
.45
.50
.55
.60
.65
1.0
2.0
3.0
4.0
5.0
Values of D/e

DIAGRAM 3

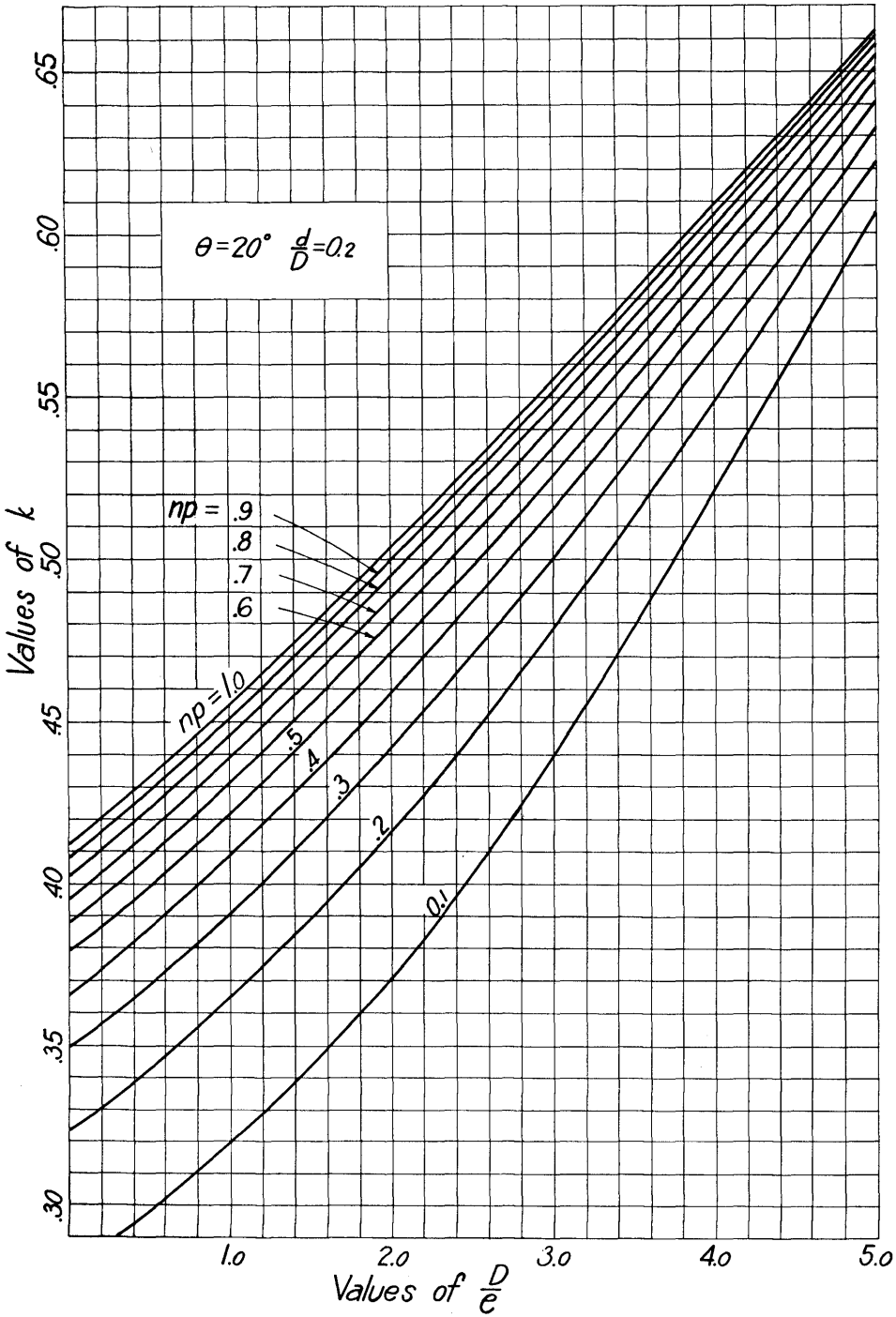
θ=20° d/D=0.2
np = .9
.8
.7
.6
np=1.0
.5
.4
.3
.2
0.1
Values of k
.65
.60
.55
.50
.45
.40
.35
.30
1.0
2.0
3.0
4.0
5.0
Values of D/e

DIAGRAM 4

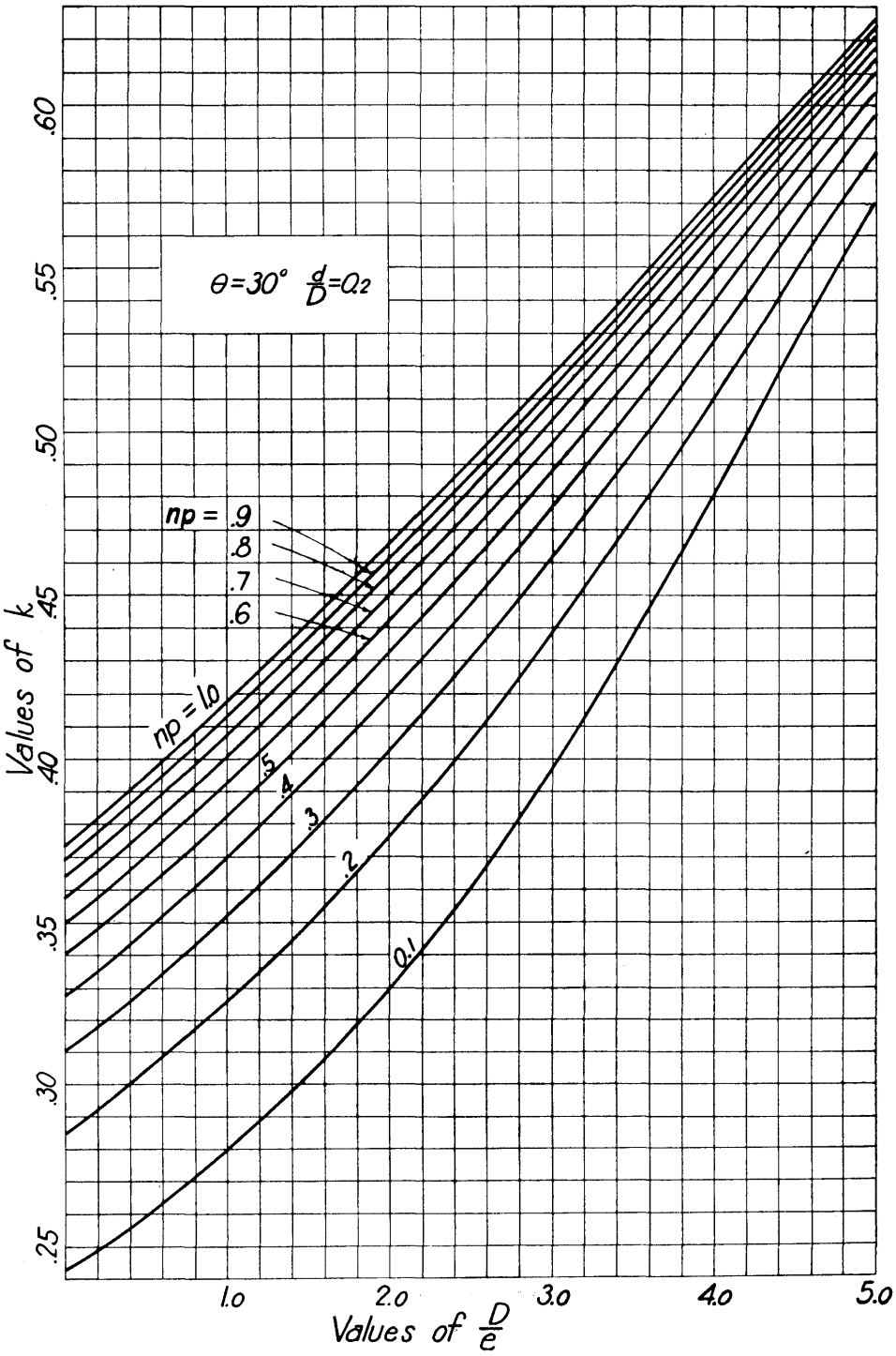
θ=30° d/D=0.2
np = .9
.8
.7
.6
np = 1.0
.5
.4
.3
.2
0.1
Values of k
.60
.55
.50
.45
.40
.35
.30
.25
1.0
2.0
3.0
4.0
5.0
Values of D/e

DIAGRAM 5

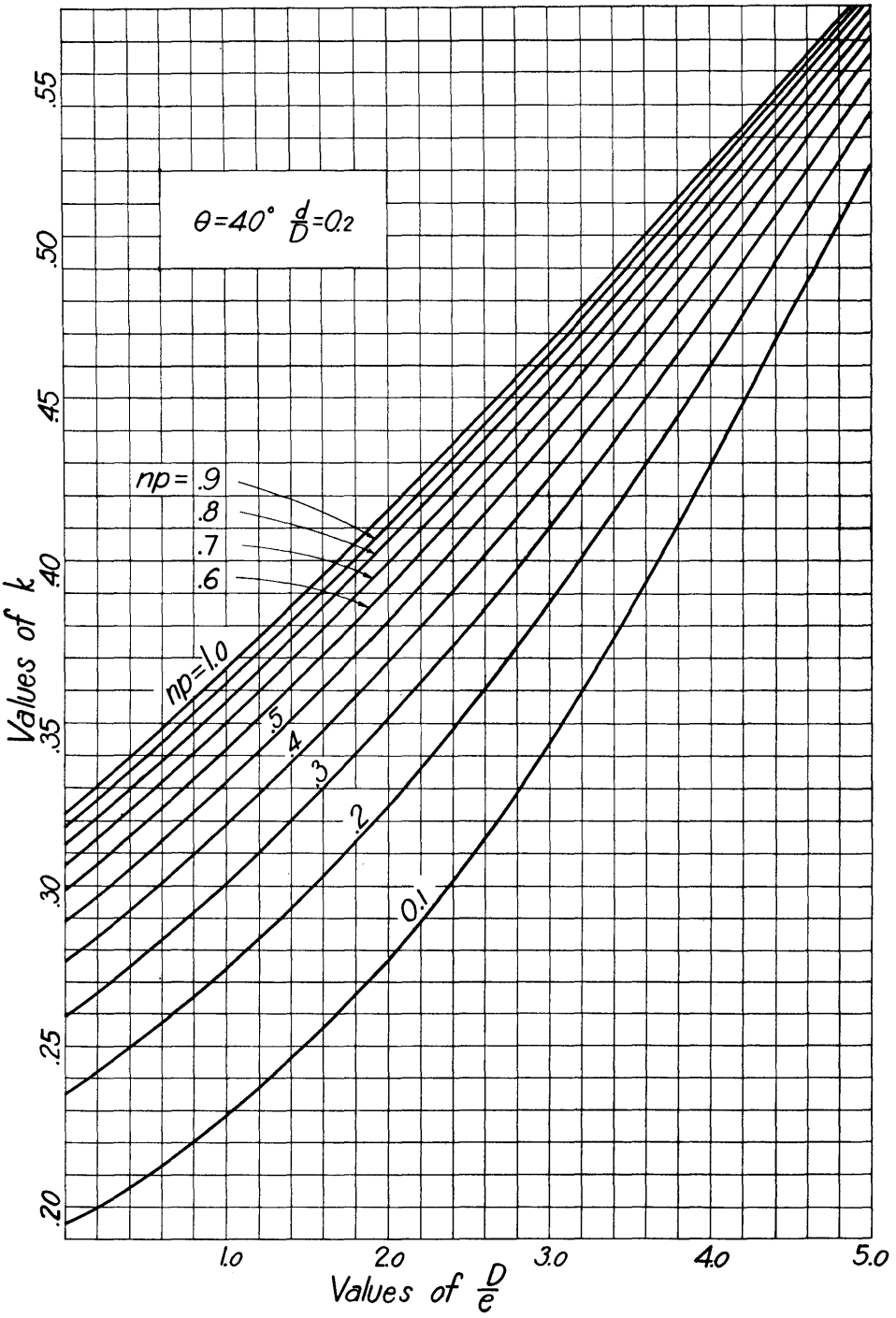
θ=40° d/D=0.2
np= .9
.8
.7
.6
np=1.0
.5
.4
.3
.2
0.1
Values of k
.20
.25
.30
.35
.40
.45
.50
.55
1.0
2.0
3.0
4.0
5.0
Values of D/e

DIAGRAM 6

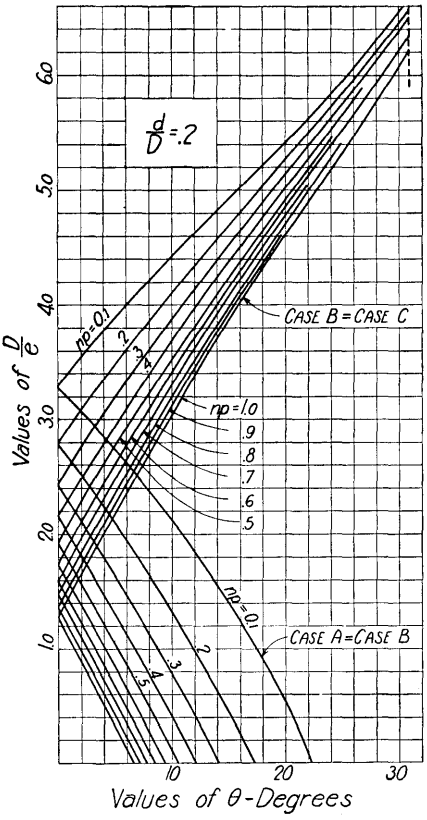

NOTE: If point determined by $\frac{D}{e}$ and θ lies below two curves, stress distribution is according to Case A; if to right of curves, according to Case B; if above curves, according to Case C.

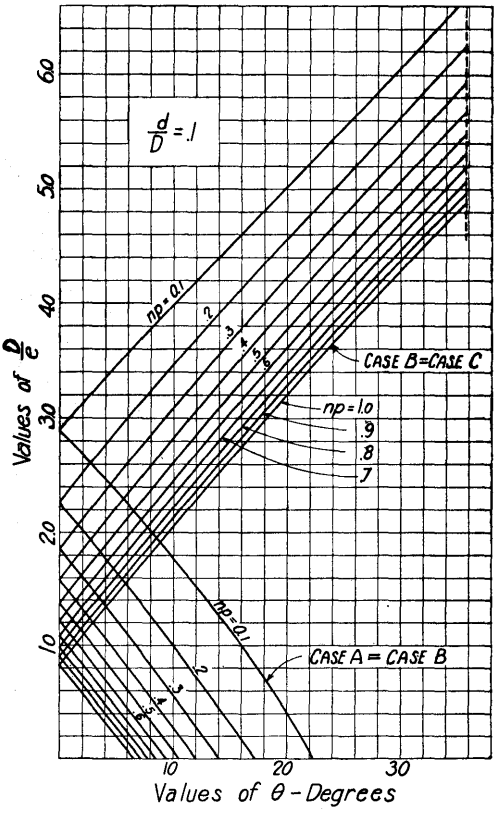

DIAGRAM 7

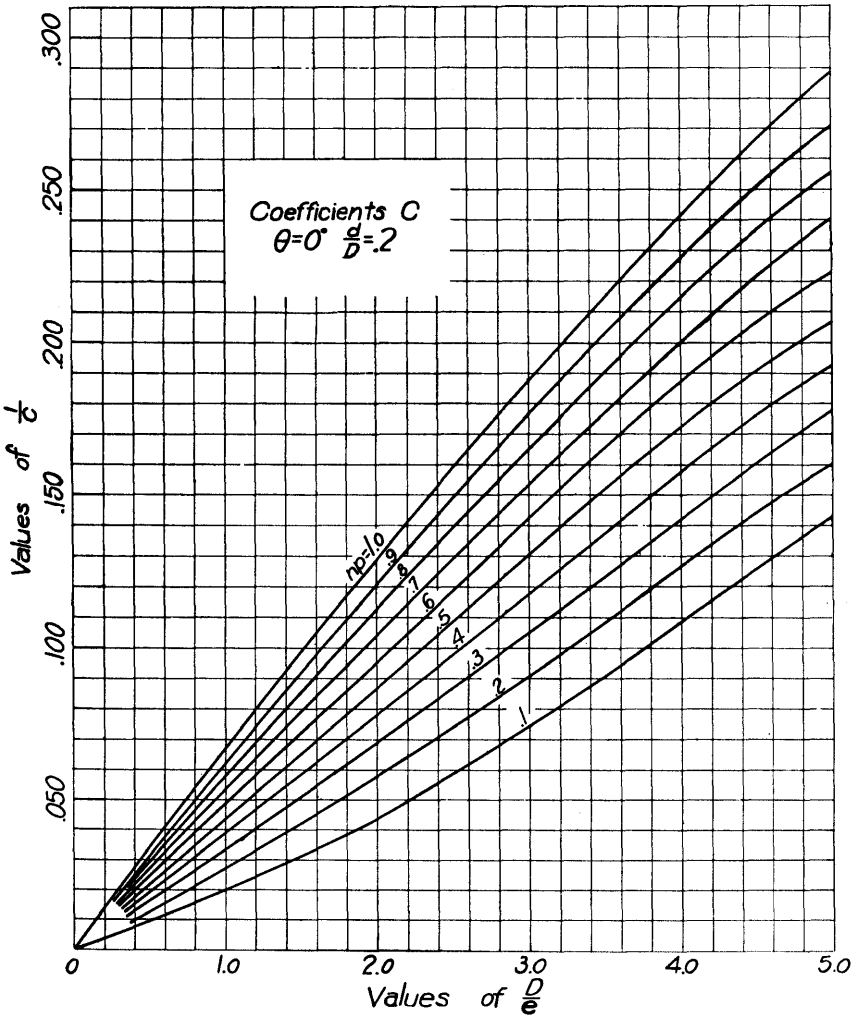
Coefficients C
θ=0° d/D=.2
np=1.0
.9
.8
.7
.6
.5
.4
.3
.2
.1
Values of 1/c
.300
.250
.200
.150
.100
.050
0
1.0
2.0
3.0
4.0
5.0
Values of D/e

DIAGRAM 8

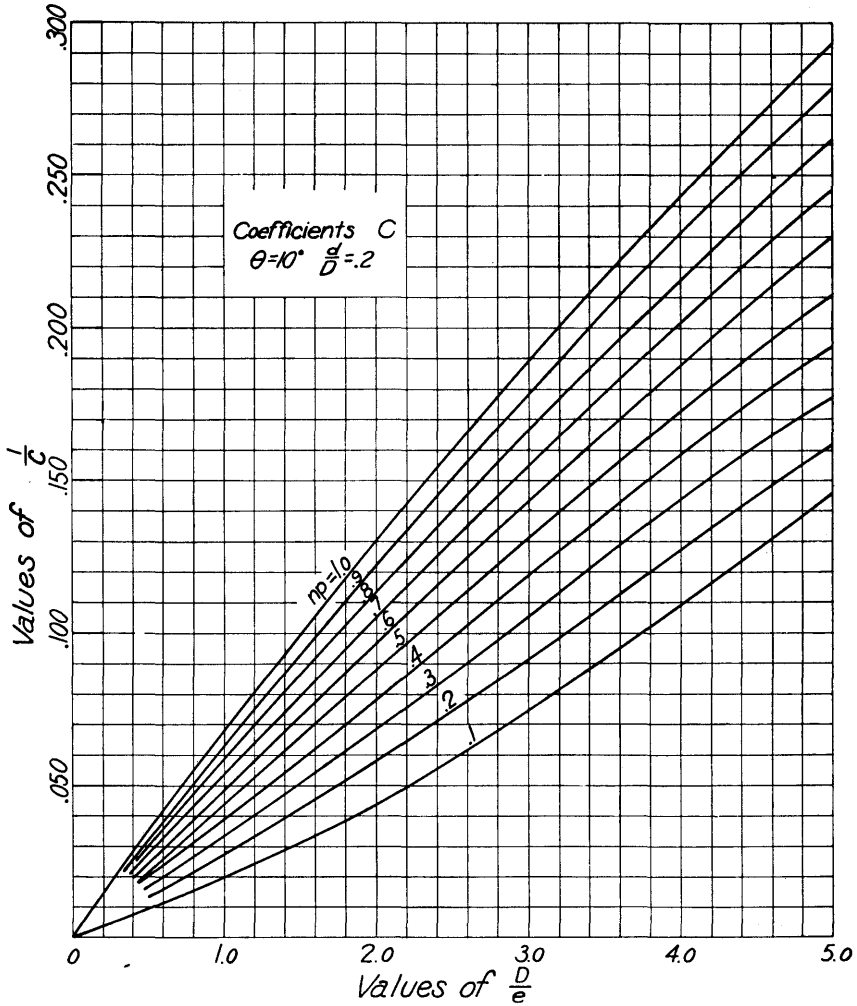
Coefficients C
θ=10° d/D=.2
np=10
9
8
7
6
5
4
3
2
1
.300
.250
.200
.150
.100
.050
Values of 1/C
0
1.0
2.0
3.0
4.0
5.0
Values of D/e

DIAGRAM 9

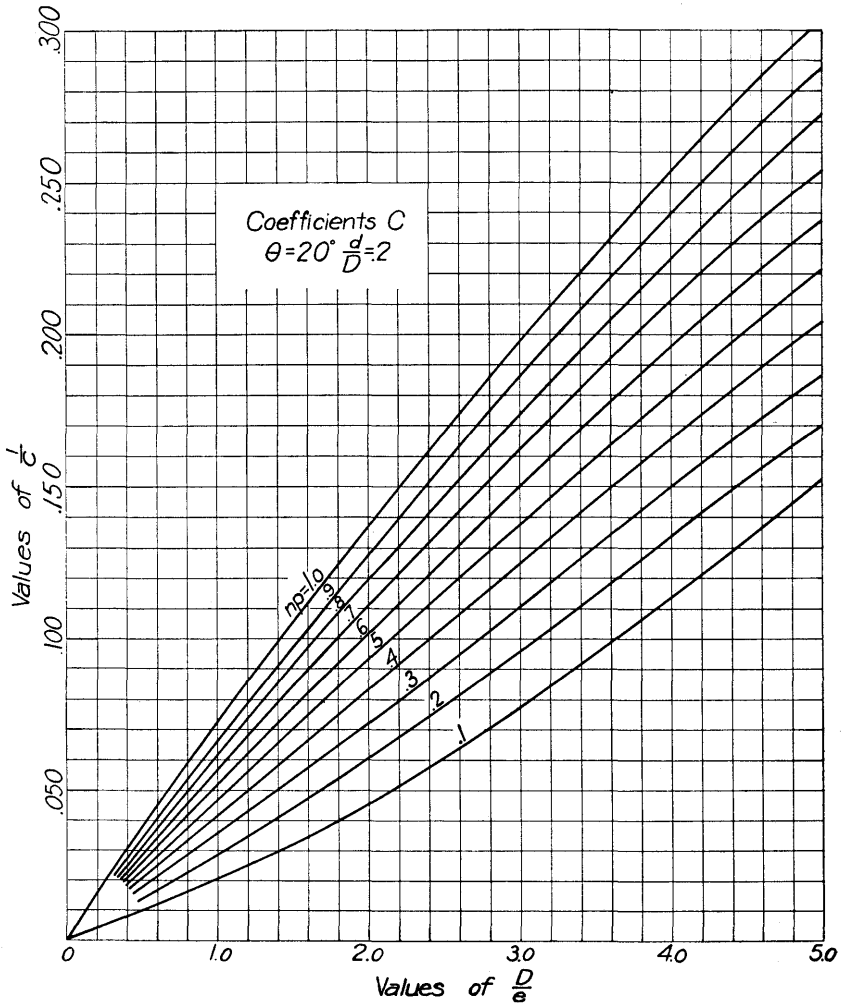
Coefficients C
θ=20° d/D=.2
np=10
9
8
7
6
5
4
3
2
1
Values of 1/C
.300
.250
.200
.150
.100
.050
0
1.0
2.0
3.0
4.0
5.0
Values of D/e

DIAGRAM 10

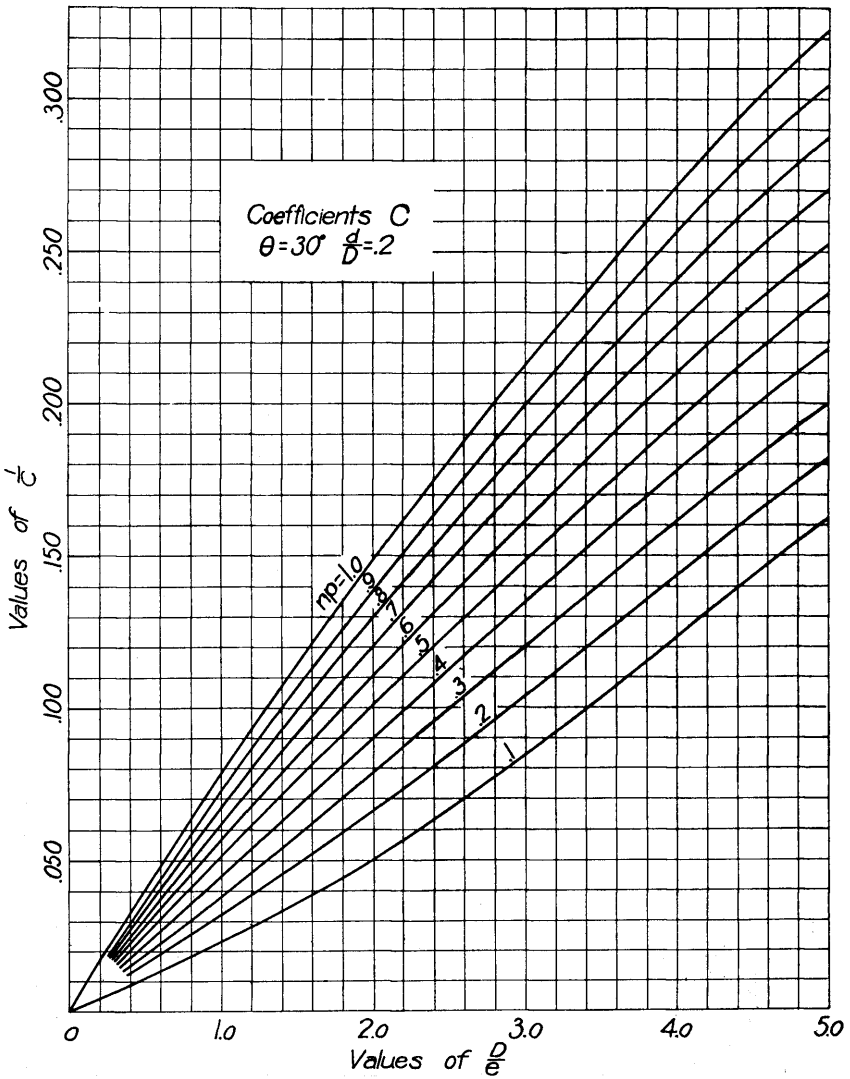
Coefficients C
θ=30° d/D=.2
np=1.0
.9
.8
.7
.6
.5
.4
.3
.2
.1
Values of 1/C
.300
.250
.200
.150
.100
.050
0
1.0
2.0
3.0
4.0
5.0
Values of D/e

DIAGRAM 11

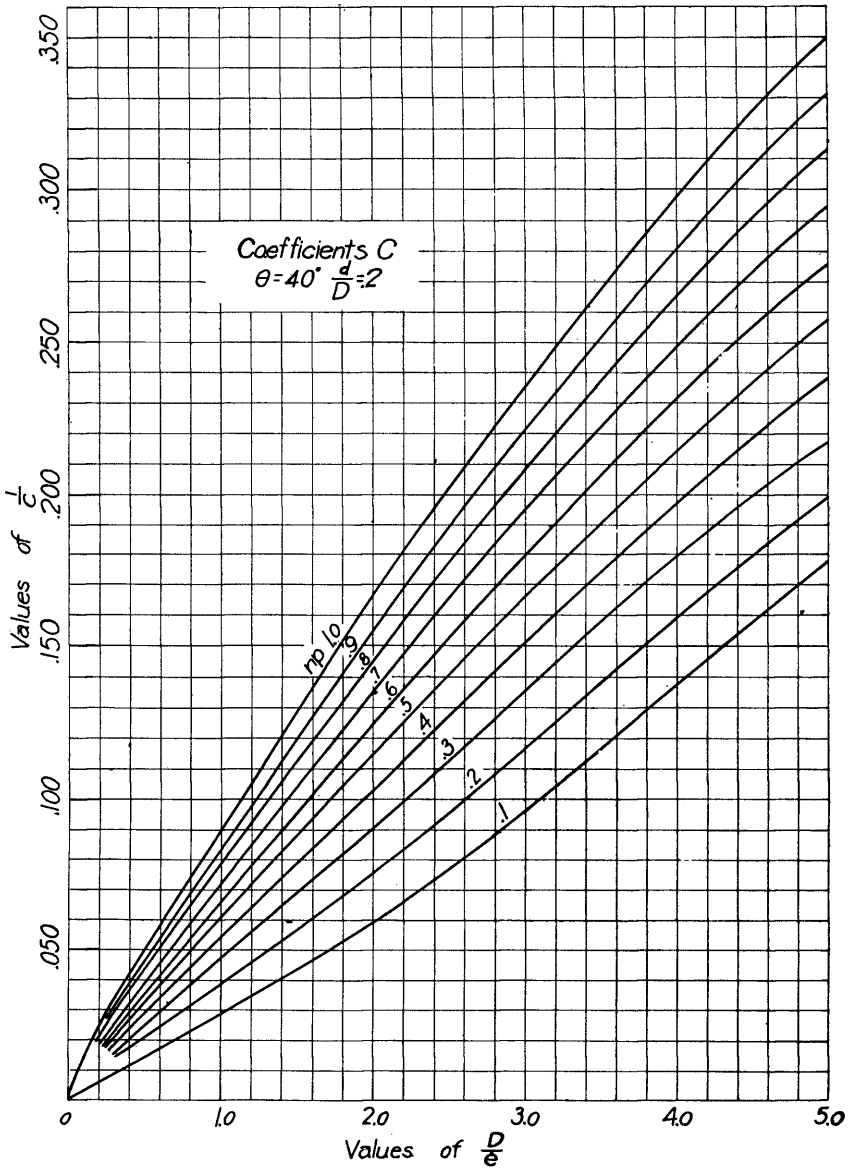
Coefficients C
θ=40° d/D=.2
rp 1.0
.9
.8
.7
.6
.5
.4
.3
.2
.1
.350
.300
.250
.200
.150
.100
.050
Values of 1/C
0
1.0
2.0
3.0
4.0
5.0
Values of D/e

DIAGRAM 12

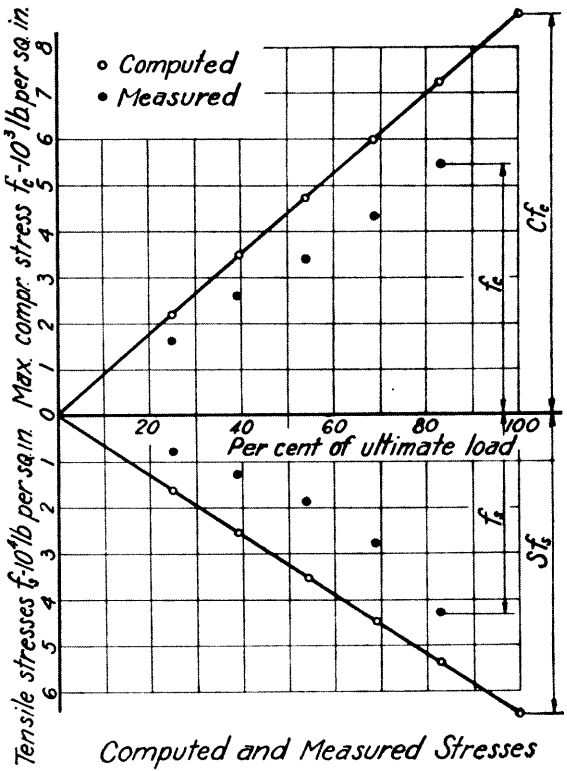

Computed and Measured Stresses
Specimen 1.

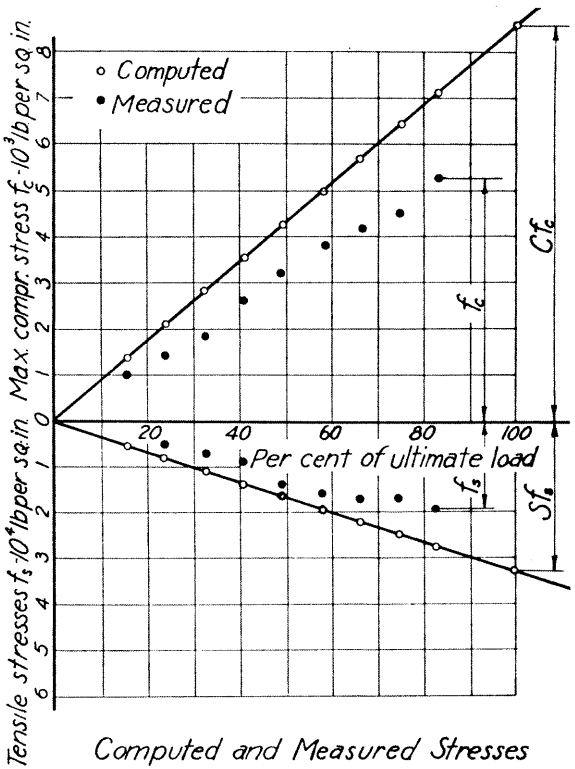

Computed and Measured Stresses
Specimen 2

DIAGRAM 13

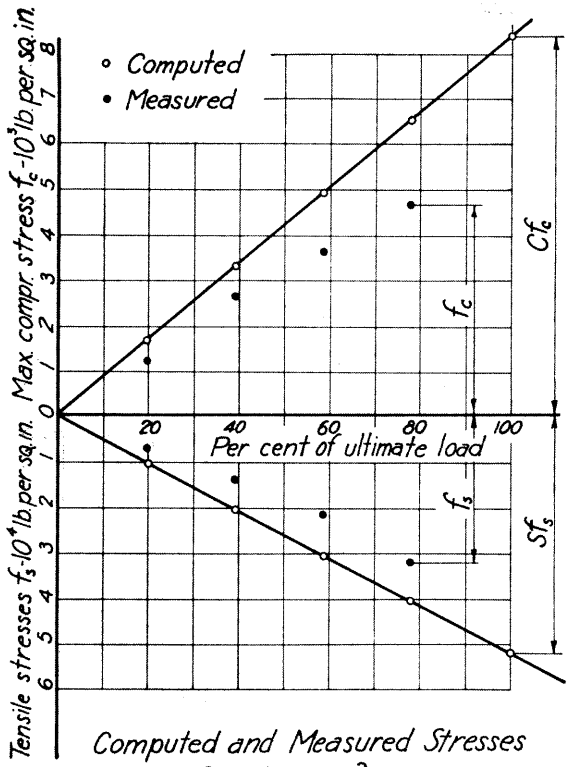

Computed and Measured Stresses
Specimen 3

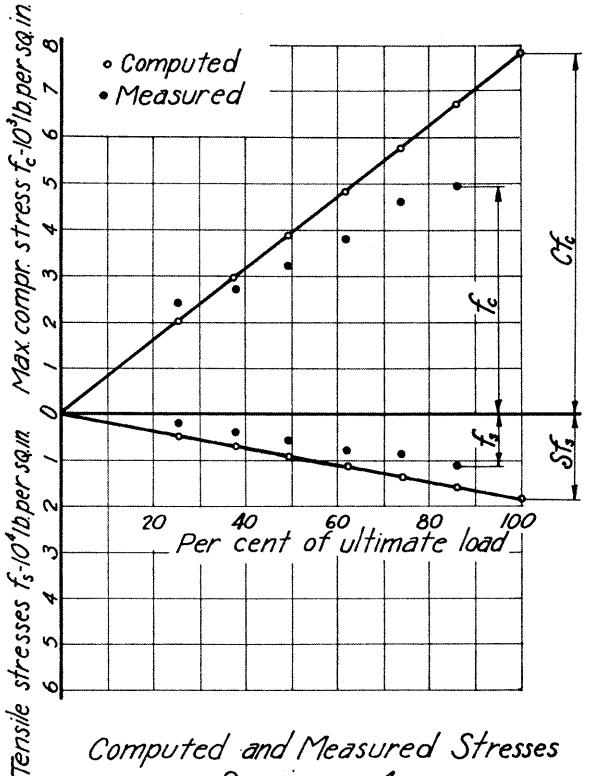

Computed and Measured Stresses
Specimen 4

DIAGRAM 14

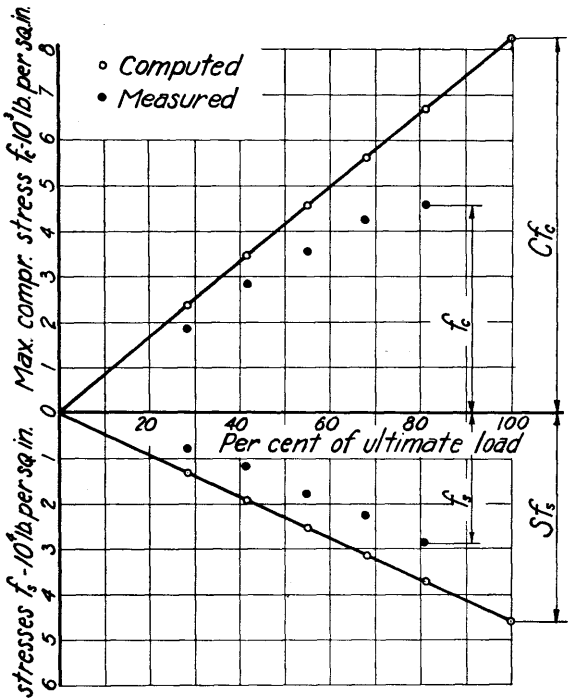

Computed and Measured Stresses
Specimen 5

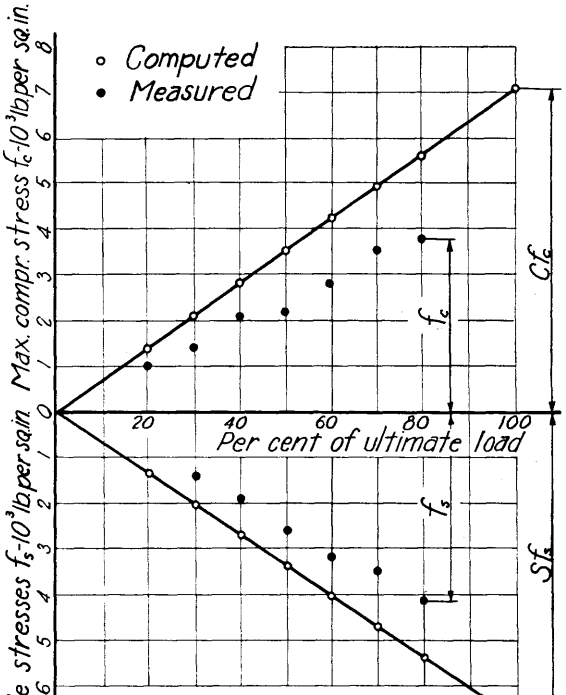

Computed and Measured Stresses
Specimen 6

DIAGRAM 15

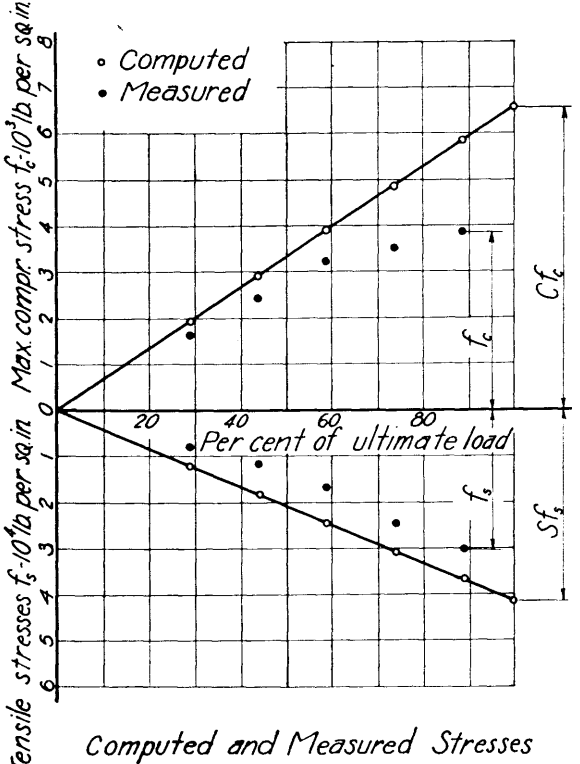

Computed and Measured Stresses
Specimen 7.

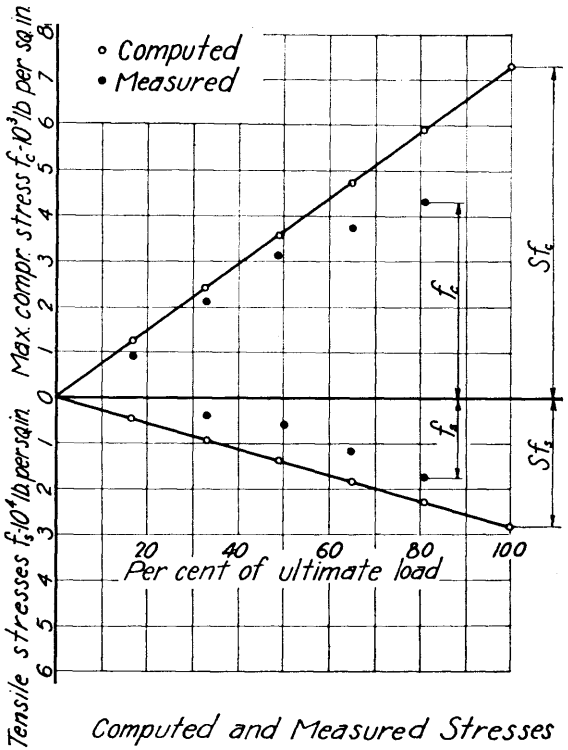

Computed and Measured Stresses
Specimen 8.

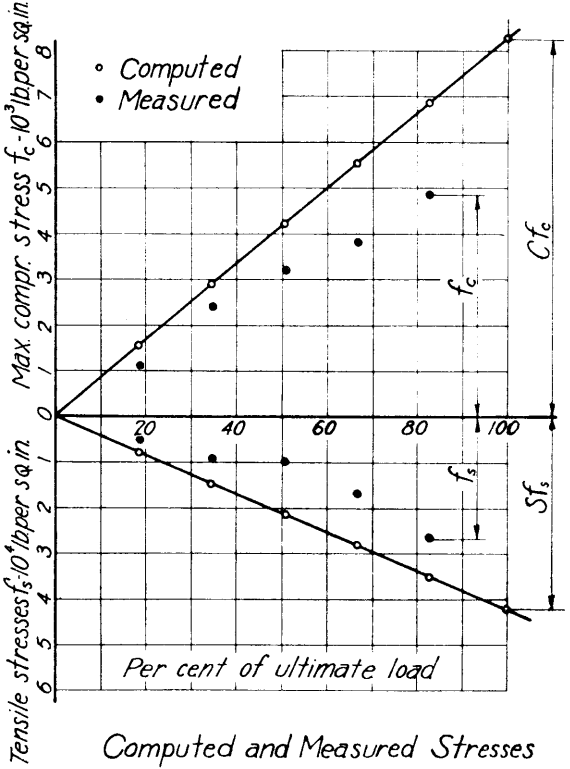

Computed and Measured Stresses
Specimen 9

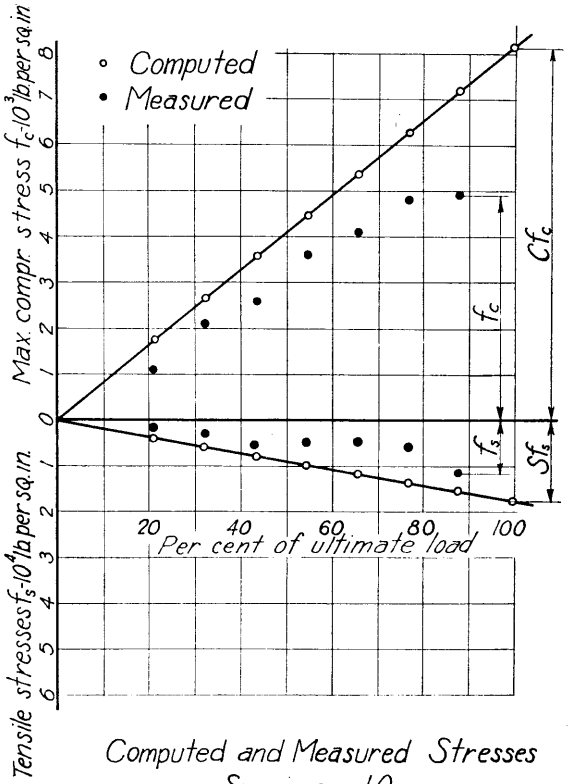

Computed and Measured Stresses
Specimen 10

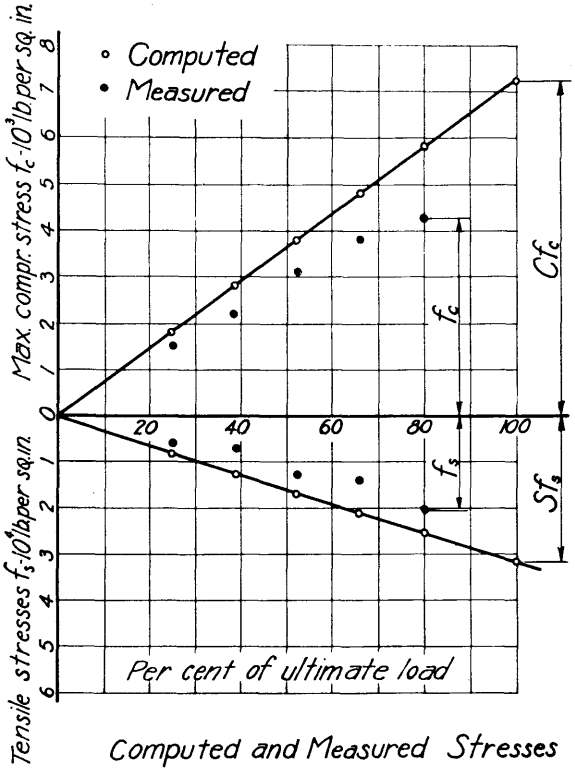

Computed and Measured Stresses
Specimen 11

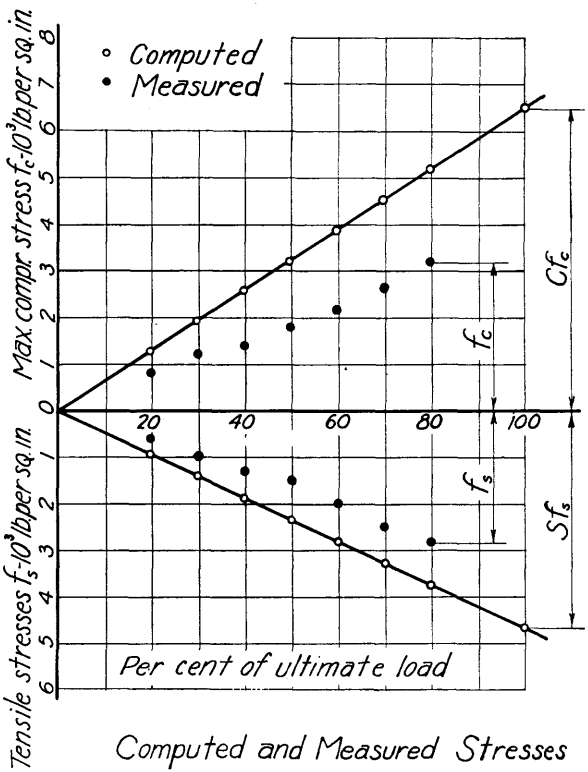

Computed and Measured Stresses
Specimen 12

DIAGRAM 18

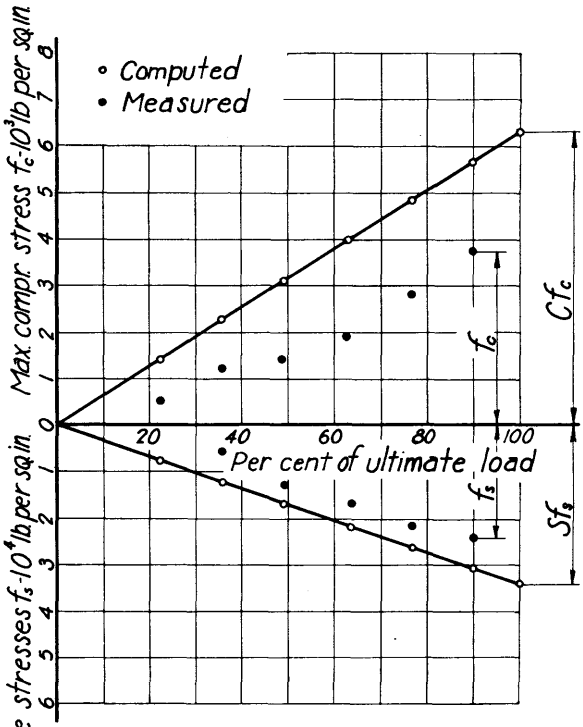

Computed and Measured Stresses
Specimen 13

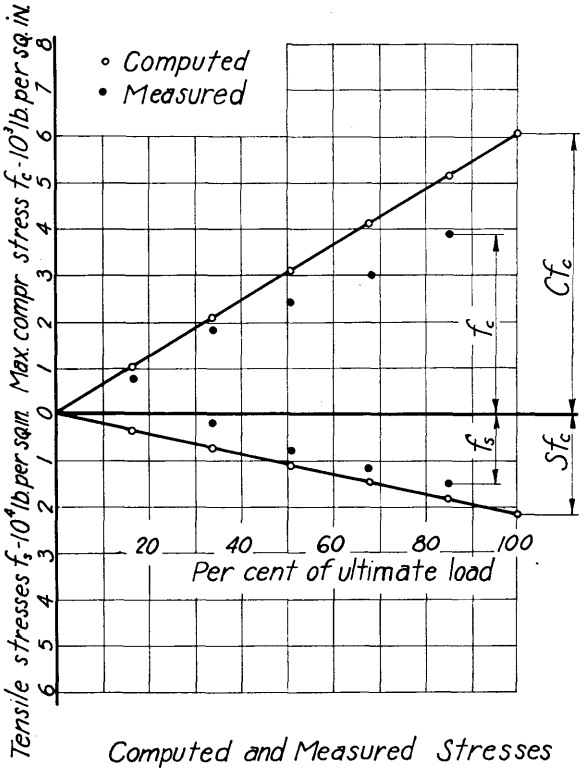

Computed and Measured Stresses
Specimen 14

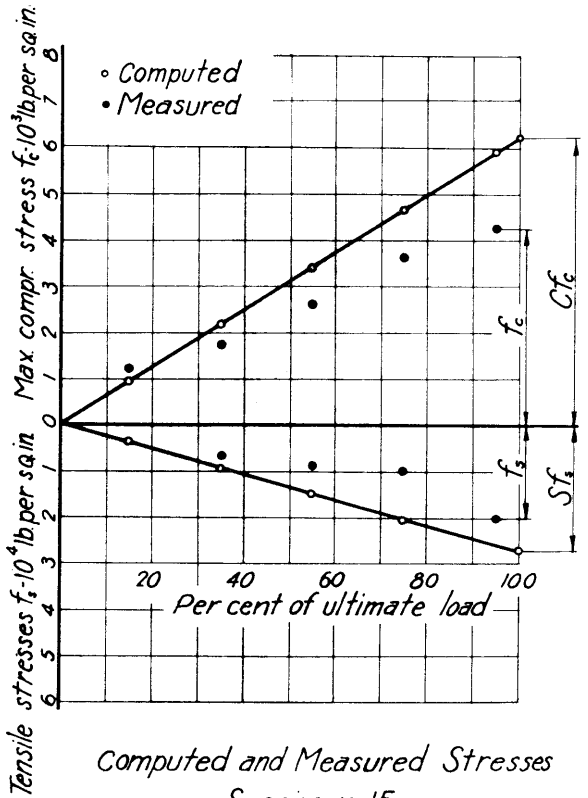

Computed and Measured Stresses
Specimen 15

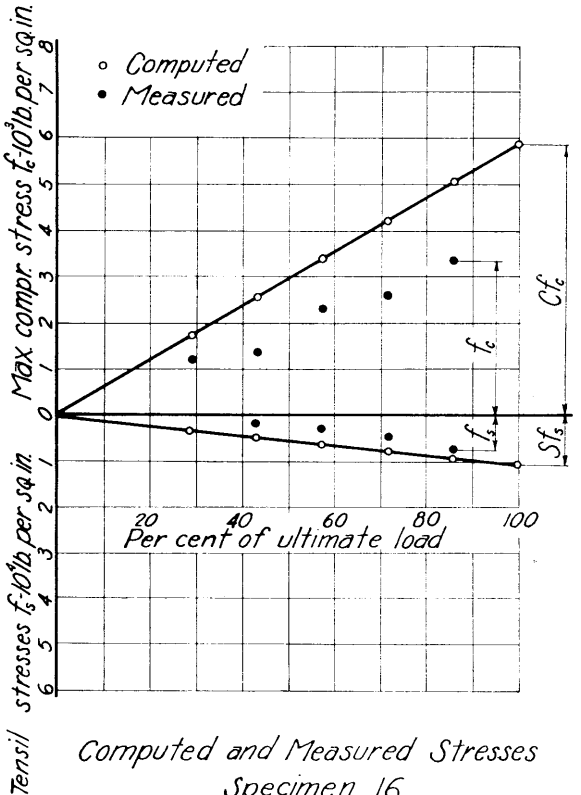

Computed and Measured Stresses
Specimen 16

DIAGRAM 20

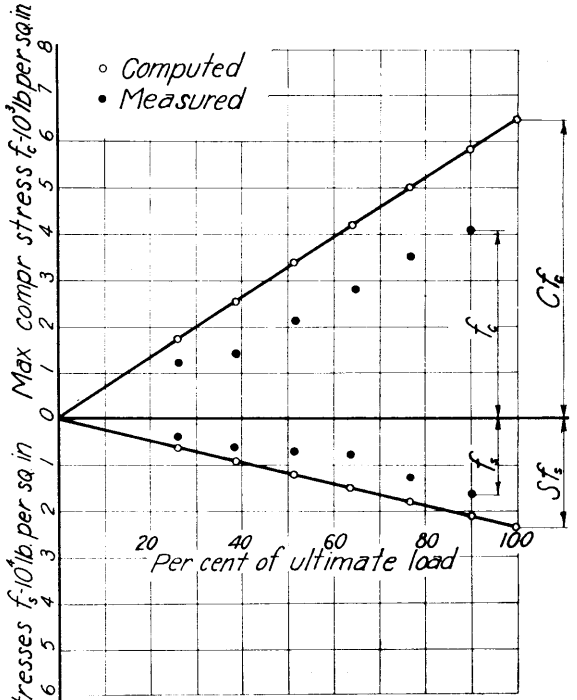

Computed and Measured Stresses
Specimen 17

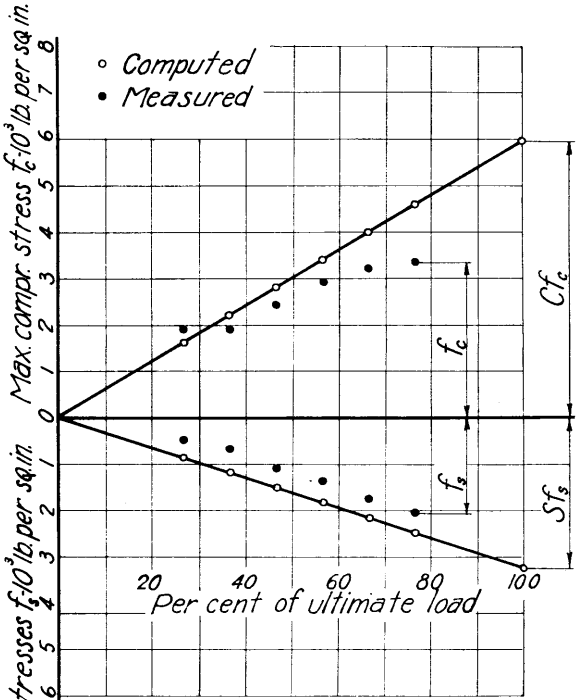

Computed and Measured Stresses
Specimen 18

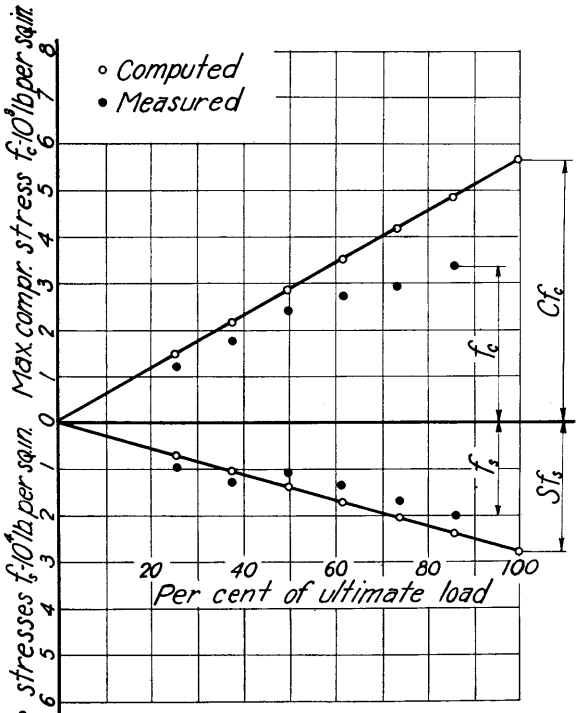

Computed and Measured Stresses
Specimen 19

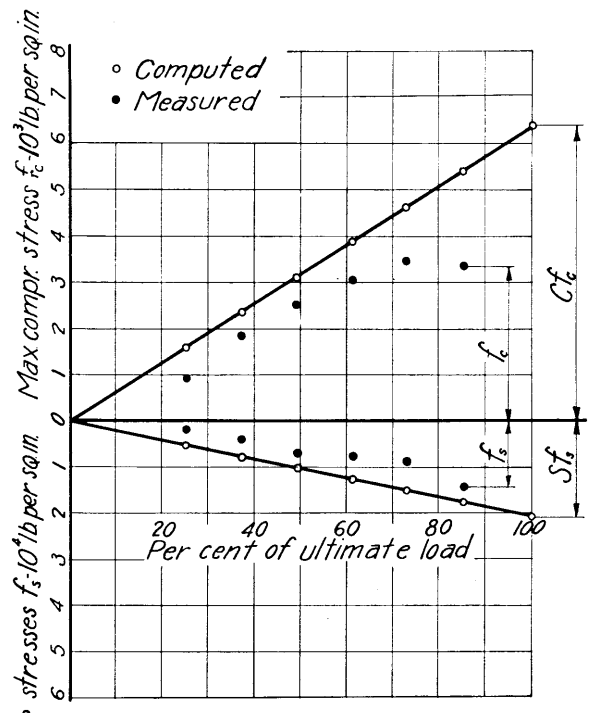

Computed and Measured Stresses
Specimen 20

DIAGRAM 22

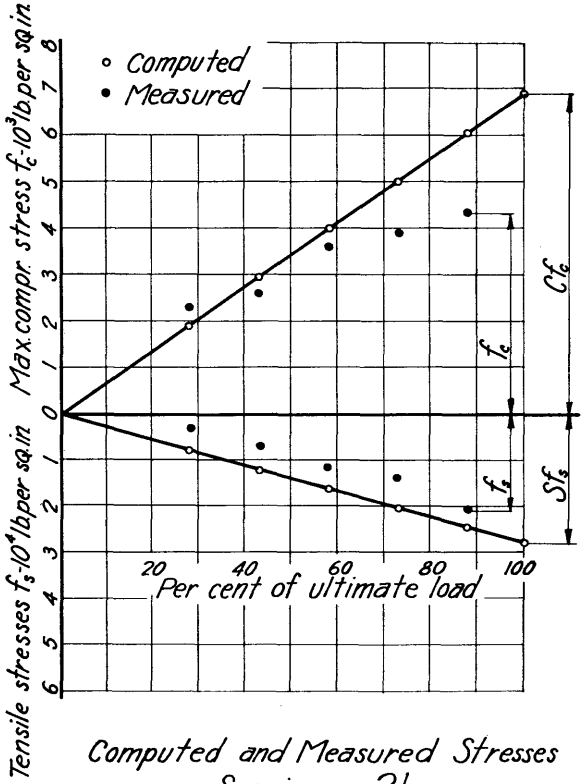

Computed and Measured Stresses
Specimen 21

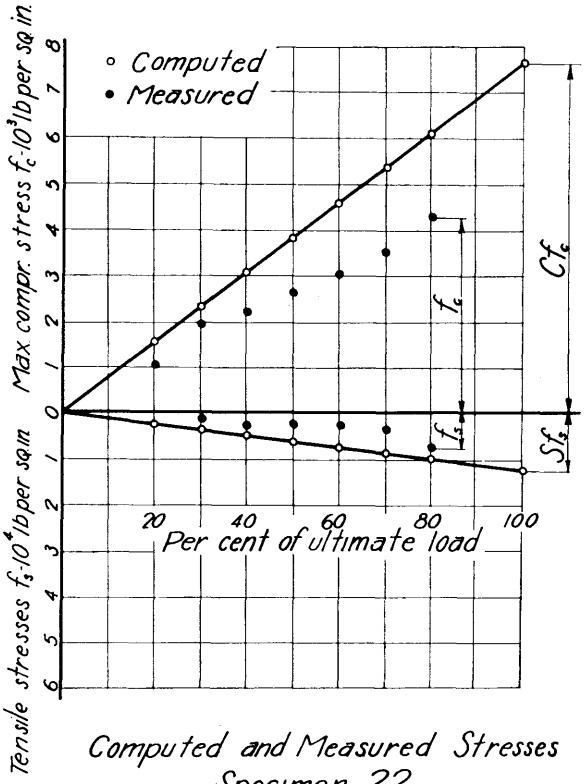

Computed and Measured Stresses
Specimen 22.

DIAGRAM 23

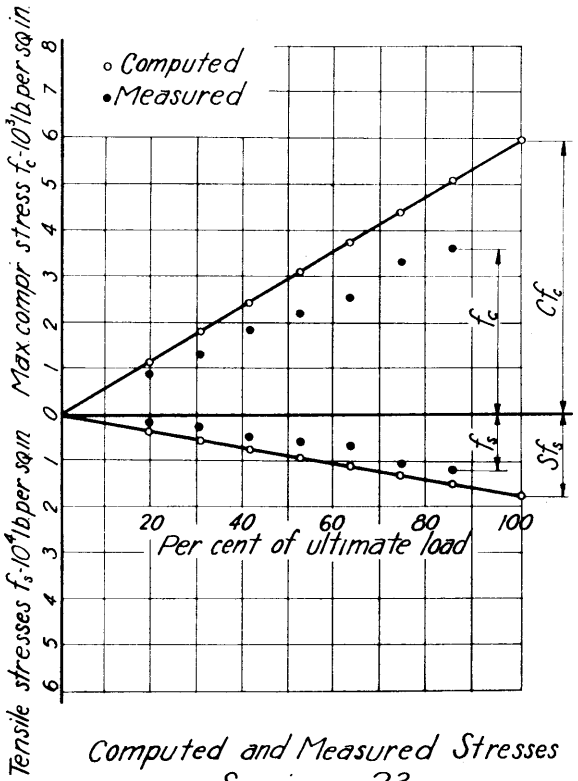

Computed and Measured Stresses
Specimen 23.

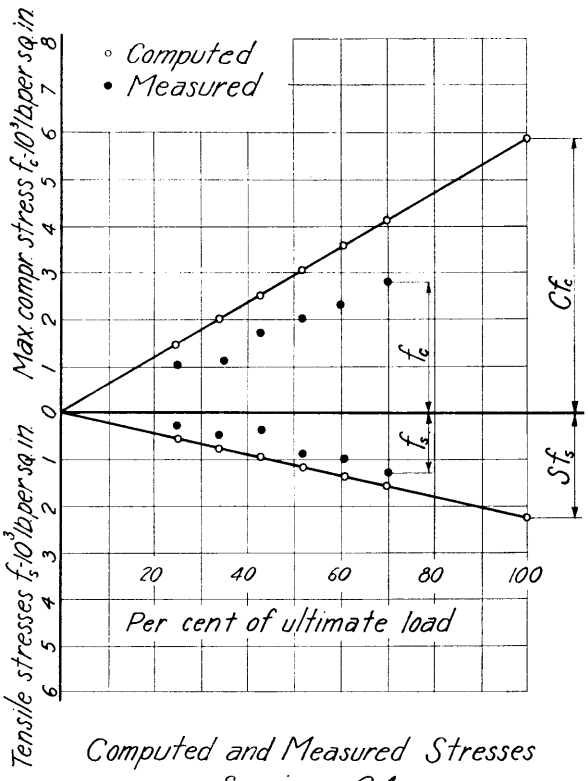

Computed and Measured Stresses
Specimen 24